

# VLCT-13 A Commercial Transport for the 21st Century

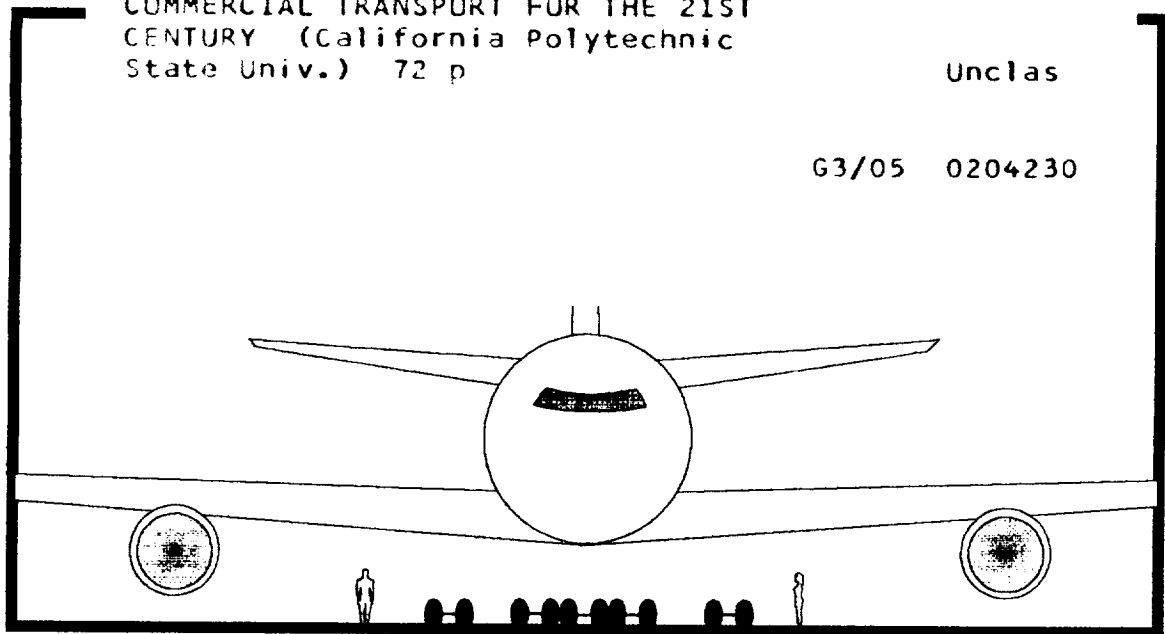
11-11-12  
204230  
P- 72

(NASA-CR-195492) VLCT-13: A  
COMMERCIAL TRANSPORT FOR THE 21ST  
CENTURY (California Polytechnic  
State Univ.) 72 p

N94-24803

Unclass

G3/05 0204230



Pamela Beal  
Terri Sowels  
Hitoshi Takahashi  
Matt Cotton  
Will Balanon  
Manuel Parayo

May 14, 1993

California Polytechnic State University  
San Luis Obispo



## **ABSTRACT**

The growth of the Pacific Rim market has spurred airframers to begin feasibility studies of a large commercial transport. By the year 2001, 30 million travelers are expected to travel the Transpacific. A transport capable of hauling 800 PAX and 30,000 pounds of cargo. 7,000 nm is of specific interest. Special problems associated with this design are configuration, landing gear, passenger safety, airport compatibility and engine thrust.

A group of students at the California Polytechnic State University at San Luis Obispo have developed very large commercial transport, VLCT-13, conventional looking design which is both comfortable and economical. Passenger comfort includes seat pitches of 34" and 40", width's of 23" and 25", respectfully, and a 27 ft diameter cross section. A direct operating cost of 2.3 cents per passenger per seat-mile is estimated for this airplane design. The airplane market price is estimated to be \$195 million 1993 dollars based on an aircraft take off weight of 1.4 million pounds. This report discusses the problems associated with the VLCT-13 and presents possible solutions.

## Table of Contents

Nomenclature.....	3
List of Figures.....	4
List of Tables.....	5
1. Introduction.....	6
1.1. Background.....	6
1.2. Market.....	6
1.3. Current Studies.....	7
2. Mission Description.....	9
2.1. Overview.....	9
2.2. Mission Profile.....	9
3. Aircraft Configuration Trade Offs.....	11
3.1. Oblique Flying Wing.....	11
3.2. Conventional with V-Tail.....	11
3.3. Conventional with High Wing.....	12
3.4. Conventional with Mid Wing.....	12
3.5. Conventional Over the Wing (OTW).....	14
4. Interior Fuselage Design.....	15
4.1. Passenger Cabin.....	15
4.2. Passenger Safety.....	18
4.3. Cargo Section.....	19
4.4. Lavatories & Galleys.....	19
4.5. Air Office.....	21
5. Cost Analysis.....	22
5.1. Operating Cost.....	22
5.2. Research and Acquisition Cost.....	23
5.3. Life Cycle Cost.....	24
6. Preliminary Sizing.....	25
6.1. Weight Sizing.....	25
6.2. Design Point.....	25
7. Wing Design.....	27
7.1. Airfoil.....	28
7.2. High Lift Devices.....	29
8. Empennage Design.....	32
8.1. Configuration.....	32
8.2. Planform Parameters.....	32
8.3. Airfoil Selection.....	33
8.4. Drag Polar.....	34
9. Propulsion System.....	36
9.1. Engines.....	36
9.2. Thrust Required.....	36
9.3. Vortex Turbine.....	37
10. Performance.....	39
10.1. Takeoff.....	39
10.2. Climb.....	39
10.3. Cruise.....	39
10.4. Descent.....	40
10.5. Landing.....	41
10.6. Performance Summary.....	41
11. Stability and Control.....	42
11.1. Static Margin Assessment.....	42

11.2. Static Stability Assessment .....	43
12. Structures .....	45
12.1. Materials .....	45
12.2. V-N Diagram .....	46
12.3. Wing .....	46
12.4. Empennage .....	49
12.5. Fuselage .....	51
13. Manufacturing .....	54
14. Landing Gear Design .....	56
14.1. Landing Gear Location and Load Distribution .....	56
14.2. Tire Selection and Wheel Arrangement .....	58
14.3. Turning Radius .....	60
14.4. Tip-over Criterion .....	61
14.5. Retraction Kinematics .....	62
15. Conclusions and Recommendations .....	64
15.1. Conclusions .....	64
15.2. Recommendations .....	64
References .....	65
Appendices .....	67

## NOMENCLATURE

## LIST OF FIGURES

1. 3-views of VLCT-13	9
2. Mission Phases	12
3. Cross Sections of Internal Layout	17
4. VLCT-13 Layout	19
5. Emergency Egress	20
6. Cargo Compartment	21
7. Laboratory Layout	22
8. Air Office Layout	23
9. Distribution of Labor Costs	24
10. Breakdown of Life Cycle Costs	25
11. T/W vs. S/W	27
12. Cast 10-2 Section Lift Coefficient vs. $\alpha$	31
13. High Lift Devices	31
14a. Horizontal Tail	35
14b. Vertical Tail	35
15. Power Operation @ 40,000 ft	37
16. Power Operation @ 36,000 ft	38
17. Vortex Turbine	39
18. Longitudinal X-Plot	44
20. Structure of Wing	48
21. Structure of Horizontal Tail	51
22. Structure of Vertical Tail	52
23. Fuselage Layout	53
24. Manufacturing Breakdown	56
25. Landing Gear Locations	57
26. Landing Gear Dimensions	64
27. Foot Print	65
28. Turning Radius	66
29. Rotation Angle	67

## LIST OF TABLES

2-1 City Pairs	12
4-1. Class Breakdown	18
6-1. Design Point Summary	28
7-1. Wing Information	30
7-2. Flap Comparison	32
8-1. Empennage Data	34
8-2. Characteristics of VLCT-13	36
8-3. Wetted Area of VLCT-13	36
8-4. Lift to Drag Ratio of Each Phase	36
10-1. Climb Performance	40
10-2. Descent Data	41
10-3. Performance Summary	42
11-1. Flight Conditions for Stability Analysis	44
11-2. Stability Derivatives	45
11-3. Longitudinal Handling Qualities Assessments	45
12-1. Aluminum-Lithium Advantages/Disadvantages	46
14-1. Nose Gear Tire Data	59
14-2. Main Gear Tire Data	60



## **1. INTRODUCTION**

### **1.1. Background**

When Boeing Company began talks with Pan Am in 1963 about an aircraft capable of carrying 300 + PAX, 5,000 + nm, the designers were confronted with problems including interior fuselage design, engines and airport compatibility. Could airports handle the passenger influx from such a large airplane? Airports were inundated with DC-10's and B-707's, the large number of passengers were already congesting the airport. The 747 would carry twice the number of people in fewer airplanes thus alleviating congestion at larger airports. Engines at the required thrust level were non-existent. Companies such as Rolls-Royce, Pratt & Whitney and GE had to design big fan engines devoting much of company's assets to this end. The interior layout required to handle 300 PAX was either thin and very long or double-deck. Joe Sutter, chief engineer of the 747 design team "...didn't like this idea on sight: to evacuate the airplane in an emergency would require escape chutes on two levels, with passengers on the upper deck facing something like an Olympic bobsled ride...".<sup>1</sup> Only until the cargo hold was designed, fitting all types of cargo containers, from truck trailers to pallets, did the 20 ft cross section for the fuselage come into play. The wide-body was ushered in for its debut, reigning supreme over long haul flights.

### **1.2. Market**

By the year 2001, 30 million passengers are expected to travel the Transpacific region.<sup>2</sup> The VLCT-13 can accommodate these passengers, assuming an daily travel of 82,000 PAX, with only 103 airplanes. These airplanes are only the transpacific fleet, a fleet of roughly the same number would be needed for trip between Europe and Asia/Pacific, 24 million passengers!<sup>2</sup> An average annual growth rate of 8% is expected in the Transpacific region between 1990 and 2001.<sup>2</sup>

"...The growth in long-haul traffic points to a need for very long range aircraft that can bypass the Tokyo bottleneck and fly from 8000-9000 stat. mi unrefueled...".<sup>3</sup> With this expected growth, a solution to crowded international airports is to develop an aircraft which can fly to any city along the Transpacific without having to stop at an in-between city. Having a long range aircraft which can also carry a large payload will also ease airport congestion.

### **1.3. Current Studies**

The growth of the airline industry and the Pacific Rim, has prompted airframers in the United States and Europe to begin a study of a 600 - 800 PAX airplane design. Boeing and European partners in Airbus began studies on the feasibility of building an aircraft of this size in January 1993.<sup>4</sup> At the California Polytechnic State University in San Luis Obispo, on the other hand, a preliminary design has been developed, Figure 1, for an aircraft capable of carrying 800 to 1000 passengers! A Very Large Commercial Transport, VLCT-13, answers the Pacific Rim demands for the 21st Century.

1.  
FOLDOUT FRAME

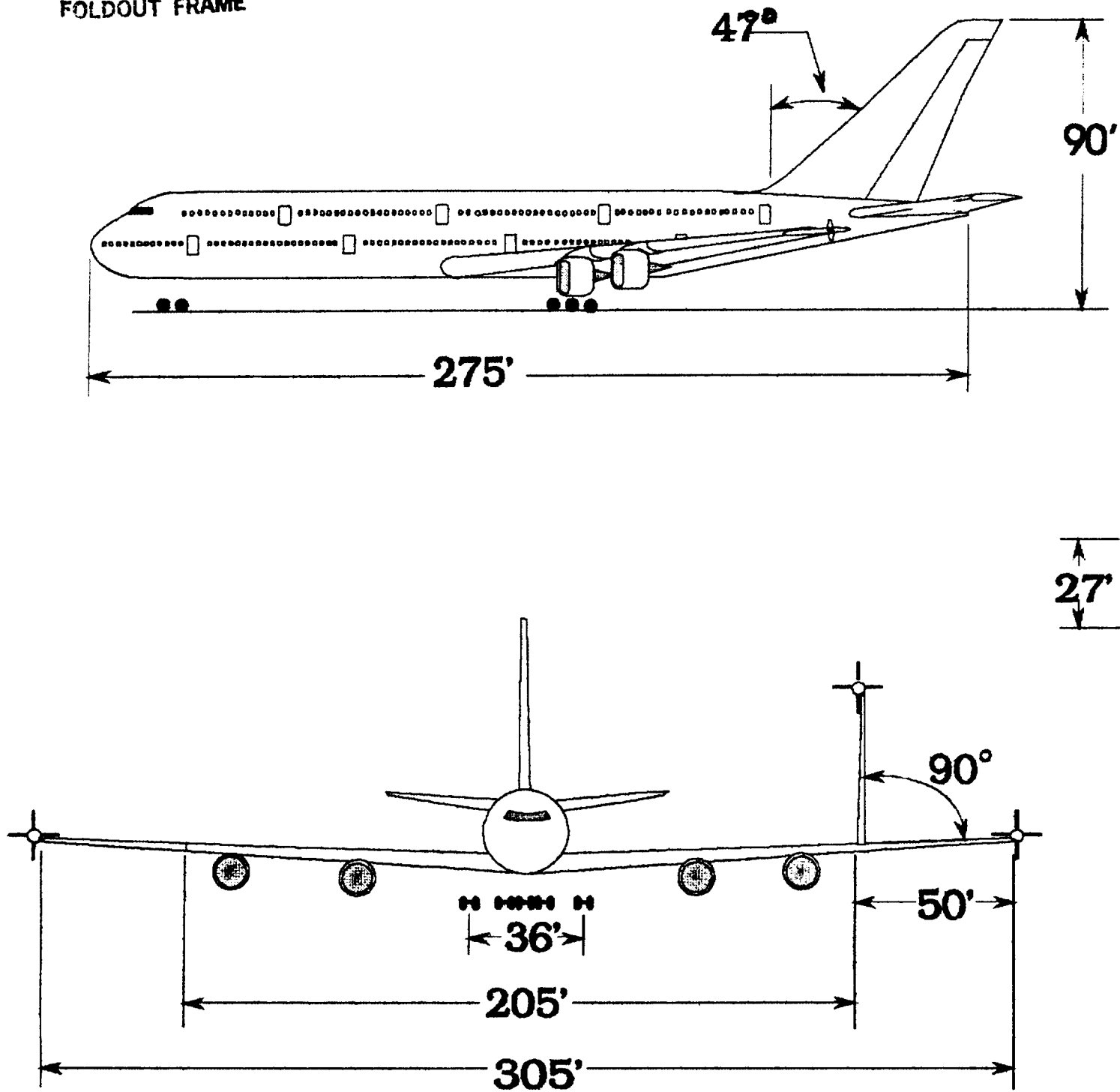
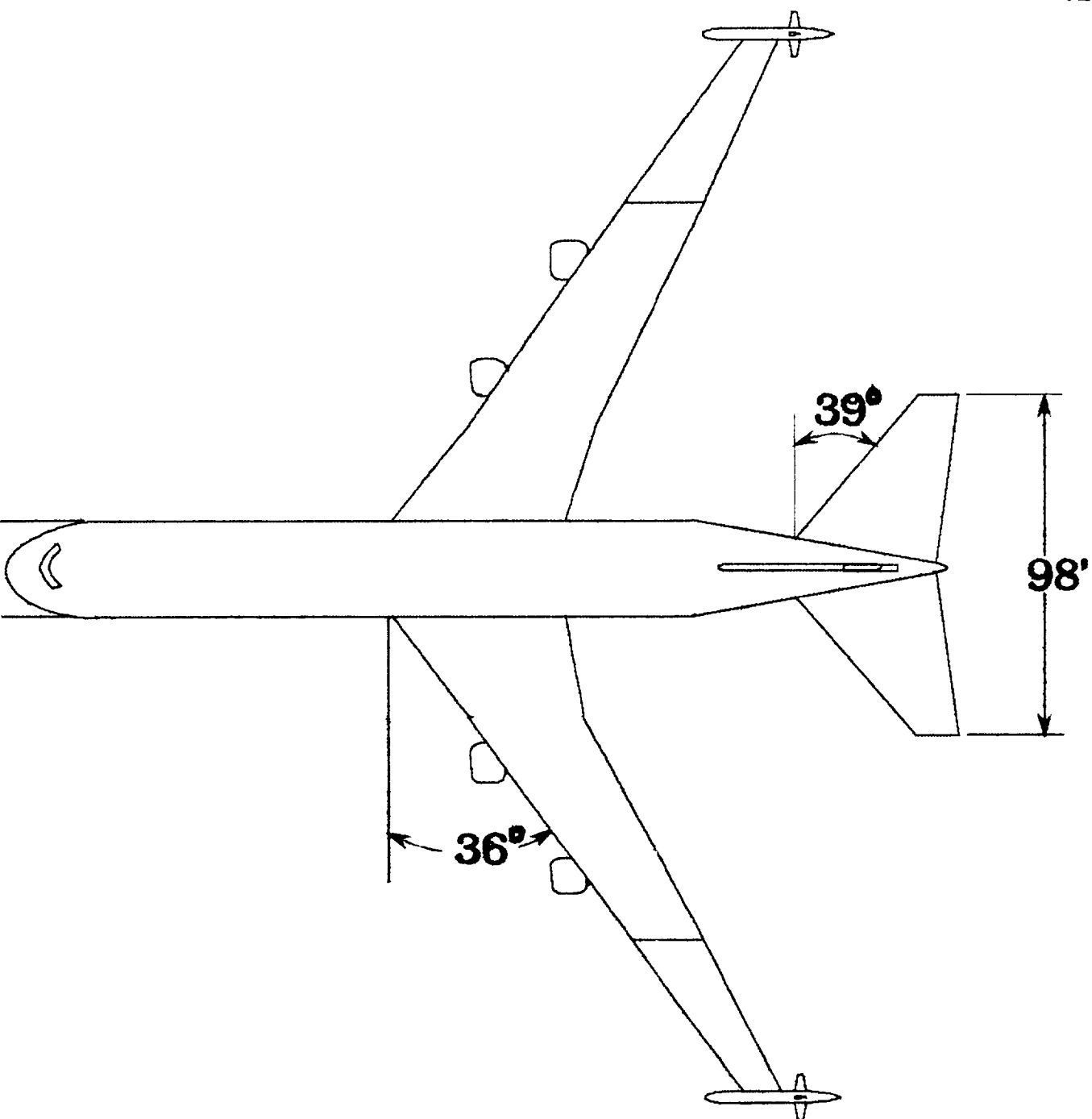


Figure 1. 3 views

2.

FOLDOUT FRAME



of VLCT-13

## **2. MISSION DESCRIPTION**

### **2.1. Overview**

A Request for Proposal (RFP) was presented to the Aerohead design team in October 1992.<sup>5</sup> The RFP centered around developing an aircraft with a passenger capacity of 800, traveling 7,000 nm carrying 30,000 pounds of cargo. A growth version capable of 1000 PAX traveling only 5,500 nm with no cargo requirement was also required. This aircraft would be a natural successor, and competitor, to the Boeing 747 series, entering service by the year 2005. The design proposal would meet or fall below FAR Stage 3 noise requirements. Also, consideration of the effect this aircraft will have on existing airports, runways, taxi ways, gates, etc. must be addressed.

### **2.2. Mission Profile**

A typical mission profile for the VLCT-13 is as follows:

1. Warm-up and taxi
2. Takeoff
3. Initial Climb; to 36,000 feet in 25 minutes
4. Initial Cruise; at 36,000 feet
5. Second Climb; to 40,000 feet in 10 minutes
6. Second Cruise; at 40,000 feet for majority of range
7. Descent
8. Loiter at 10,000 feet if necessary
9. Land
10. Taxi into gate

See Figure 2 for a visual representation of the mission profile.

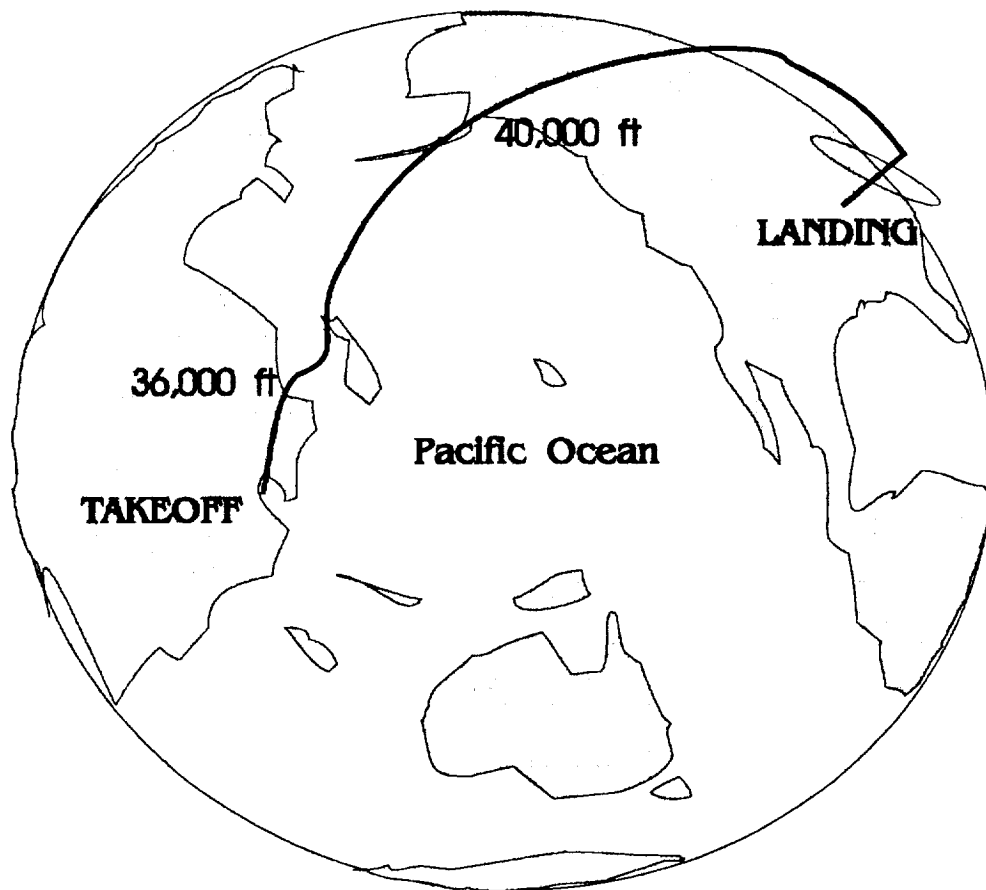


Figure 2. Mission Profile

The VLCT-13 has the capacity for ranges up to 7,000 nm, so an individual mission will have its own profile. The above list is a generalized case, each mission contains elements of each step. For example, the overall range may be different, but the Second Cruise will always be the longest phase of the VLCT-13 mission.

A typical Pacific Rim mission would be LA to Tokyo, 5,000 nm. Other possible city pairs are listed in Table 2.1.

Table 2.1. VLCT-13 City Pairs

City Pair	Range (nm)
LA - Sydney	6500
Chicago - Hong Kong	6800
San Francisco - Singapore	6800
Amsterdam - Jamaica	5000

### **3. AIRCRAFT CONFIGURATION TRADE OFFS**

#### **3.1. Oblique Flying Wing**

The flying wing is gaining popularity as evidenced by the B-1 bomber and NASA studies.<sup>6</sup> The oblique flying wing is a Supersonic Transport configuration. The flying wing would take-off with only about a  $30^\circ$  sweep. As the wing accelerates, more sweep is added resulting in a  $60^\circ$  oblique flying wing.<sup>7</sup> One interesting advantage of the flying wing was the possibility of converting to a supersonic aircraft, at some future date, and offering this as a growth version.

An unusual configuration was desired for the challenges involved such as landing gear, passenger egress, flight deck vision and stability and control. Each of the landing gear would have to be steerable so the airplane could turn onto the taxi way and runway. Placement of the landing gear on the airplane to not only fit on existing runways but also to distribute the weight evenly over the pavement. Passenger egress was a major problem. There was no way to meet FAR 25 requirements. Doors would have to be located on the leading edge and trailing edge of the wing. Along the trailing edge, stairs would have to be used so that passengers would climb out. An elderly person or physically disabled person would not be able to climb the stairs; stair would constitute an obstruction. FAR 36 vision requirements from the flight deck could not be met without the use of optical imaging systems. The pilot's line of sight would not meet the  $45^\circ$ , or  $135^\circ$  requirement without the use of camera's. The airplane requires a large amount of stability and control augmentation to achieve good handling and ride qualities; augmentation systems can become very expensive.

The oblique flying wing configuration presented too many problems and could not be justified as a viable configuration.

#### **3.2. Conventional with V-Tail**

A conventional airplane configuration of this large size would require a vertical tail that would be too tall. New hangers would have to be built accommodating this airplane for maintenance. An idea of attempting to shorten the vertical tail by designing a V-tail. By lowering the overall height of the tail section, better maintenance accessibility and decreased drag would be achieved. Sizing the V-tail resulted in the same surface area as a conventional tail and shortened the height. Drag increased. As drag began to increase, the

required high L/D decreased, resulting in an airplane that would never fly. More structure would be required in the aft section to handle the V-tail. This concept was discarded.

### **3.3. Conventional with High Wing**

The installed diameter of the big fan engines required by this aircraft are 12 ft. Providing enough distance between the fan and the ground to minimize FOD ingestion would require tall landing gear. At this preliminary stage in the design process, landing gear length was high enough that current passenger gates would not reach the loading door. Using a high wing would move the engines high enough off the ground to protect from FOD and decrease landing gear height.

A problem arose involving placement of the wing box through the fuselage. The wing box was estimated to be about 6 ft thick at the fuselage. Without creating a large "bump" on the top of the airplane, this 6 ft would have to be taken away from the upper deck passengers. Roughly a 40 ft length of passenger space would be the wing box. This arrangement would be inconvenient; passengers would have to walk down to the main deck and then climb stairs to get to their seats, compromising passenger comfort.

The primary market for the VLCT-13 is the Pacific Rim; there is a lot of ocean between the United States and Asia. If VLCT-13 crashes into the ocean, the fuselage would be under water because of the high wing. With the fuselage under water, the passengers would have no way to safely evacuate the airplane: a hazard that could not be ignored. If the VLCT-13 crashed on landing, the rigid wing box was useless and the fuselage would break up, killing the passengers: compromising passenger safety.

From a safety and passenger comfort standpoint, a high wing configuration would not work.

### **3.4. Conventional with Mid Wing**

The conventional mid-wing design was considered for three reasons. First, to increase the engine height above the ground without making them unreachable by maintenance crews. Second, to decrease the interference drag between the fuselage and the wing. Third, to decrease the length of the landing gear so the loading door could be at a compatible height to current airports.



If the mid-wing design were implemented, the engines would certainly be safe from FOD. The height of the bottom of the engine from the ground would be anywhere from 5 ft. to 9 ft. above the ground depending on the placement. This range goes from the engine positioned right next to the fuselage to 57 ft. out from the fuselage centerline. So, it would have the added benefit of being able to place the engines closer to the center of mass, lessening any yawing moments created with one engine out situations.

A mid-wing would also be better for drag reduction. With the wings protruding out of the fuselage at 90 degree angles, the interference drag is less than with a high or low wing aircraft. But, the major problem with this is the wing box. In the case of the VLCT-13, the wing box at the root is 6 feet thick. this creates a lot of difficulty in creating a safe haven for our passengers. The wing box would be located on, and in the main deck of the airplane. This would make passengers that are to be seated in the rear of the plane load in the front, go up the stairs to the upper deck, then go down some back stairs to their destination. Another drawback is the loss of seats, it was estimated that the wing box would replace 100 passengers. In order to make our 800 PAX quota, the plane would have to be lengthened, increasing airport compatibility problems., not to mention the fact that there would be fuel running in front and behind passengers. This was considered to cause a slight uneasiness with potential passengers. What gave the designers some uneasiness, was that in the event of a water crash, the water line would be up to the wing, hence the main deck would just be under the water line. This would hinder the emergency doors on the entire main deck useless. This was seen as the major factor in declining to use the mid-wing design.

But what if the passengers couldn't get onboard because the loading door is too high for the gate to reach? This was a problem that was worked out by increasing the dihedral slightly and positioning the wings farther out on the wing. Doing these things left us with a moderate FOD concern and a loading door that can be reached with a conventional gate.

The mid-wing was considered for its reduced drag potential and decreasing the risk of FOD. But, the thing that killed it was the fact that passengers would feel unsafe. It was felt that the mid-wing is a good design if you are carrying cargo, not passengers.

### **3.5. Conventional Over the Wing (OTW)**

The OTW concept was considered to help with FOD and also help with flow attachment over the wing. It was felt that an engine on the wing could not contribute a significantly more amount of drag than a snug under the wing engine. After some research was made, we determined that the assumption was wrong. It was found that an OTW arrangement can give an increase of 40% in lift-dependent drag.<sup>8</sup> This number is just too high for the VLCT-13 to handle in a cruise at 40,000 feet. Another reason to discard this design, is that the VLCT-13 readily makes its RFP takeoff length requirement. OTW designs would be worth while looking into if the airplane was not meeting its takeoff or landing field length requirements because the lift coefficient is increased dramatically. Another obstacle to overcome is the maintenance and safety aspects. Because the engine would be placed on top of the wing, maintenance crews might damage the wing if tools were dropped. If the engine needed to be dropped in an emergency, then the engine would take the wing with it. This was considered as undesirable to the design team.

## 4. INTERIOR FUSELAGE DESIGN

### 4.1. Passenger Cabin

A philosophy of "passenger comfort for an economical price" was decided upon early in the design phase. Currently, TWA runs television commercials selling more leg room.<sup>9</sup> A USA Today report showed that 42% of international passengers are willing to pay the extra cost of Business class.<sup>10</sup> An airplane which offers comfort for an economical price would be a success.

There are not any aircraft of this size on the market. What has been done before in regards to interior design before can now be changed. Instead of trying to pack as many PAX as possible into an airplane, designers can develop an arrangement which is both comfortable physically and emotionally. The wide open space of the interior should not be marred by being cheek to cheek with a neighbor. The VLCT-13 was expected to have a large wing span and large fuselage; what is the point of limiting seat size to the current sardine arrangement. With a large aircraft, interior designers finally have an opportunity to design comfort. The VLCT-13 offers this comfort. There are two variations of class breakdown for the VLCT-13: a Tri-Class and a Dual-Class, Table 4-1. The tri-class contains the usual 1st class section. Business 1st is the VLCT-13 business class. Business class is a tourist class for the 21st Century. Figure 3 shows a cross section of this arrangement.

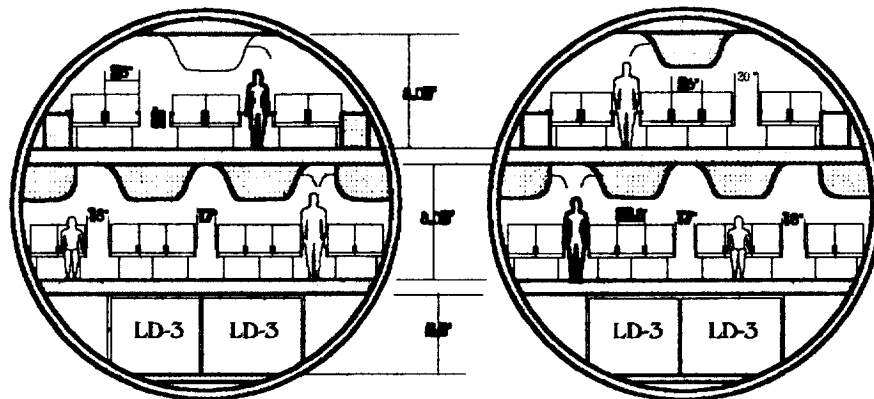


Figure 3. Cross Sections of Internal Layout

For international and domestic travel, most airlines offer a tri-class seating arrangement: first class, business class and economy (coach) class. The VLCT-13 offers such a tri-class arrangement, Table 4-1. This

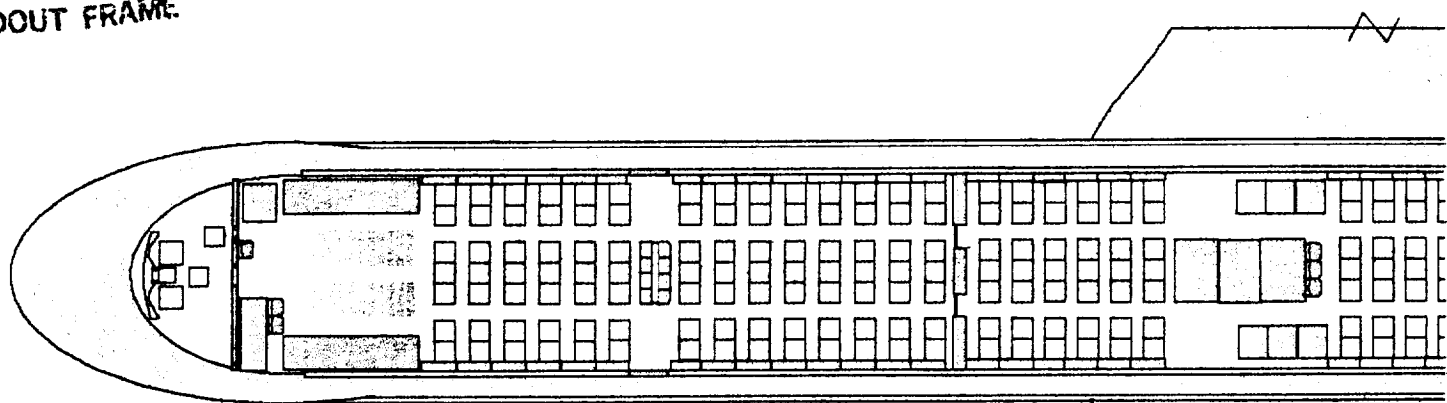
breakdown of classes was determined from Boeing 777 and MD-12 documents.<sup>11,12</sup> The VLCT-13 offers seat comfort. The First class seats can be reclined to simulate a bed. For the two class arrangement, the upper deck is exclusively Business First passengers, Figure 4. This particular interior arrangement was seen as optimal by the design team because there were too many first class seats in the tri-class arrangement to economically justify if only 8% of international passengers travel 1st class.<sup>10</sup> Besides, with such a large Business 1st seat pitch, air travelers can get the luxury of 1st class for a Business class rate.








Table 4-1. Class Breakdown

<b>Class</b>	<b>Seat Dimension</b>	<b>Tri-Class</b>	<b>Two-Class</b>	<b>Growth Version</b>
First	28" x 60" pitch	60 PAX	none	none
Business 1st	26" x 40" pitch	168 PAX	266 PAX	96 PAX
Business	23" x 34" pitch	586 PAX	586 PAX	none
Economy	20" x 32" pitch	none	none	916 PAX
		<b>Total - 814</b>	<b>Total - 852</b>	<b>Total - 1012</b>

In the VLCT-13 growth version, expanding to 1000 PAX meant giving up some comfort. The seat decreases to a 20" x 32" pitch arrangement. Doing this permitted the additional number of passengers required. In fact an all tourist class arrangement was 1084 PAX! The VLCT-13 will accommodate 96 Business 1st class and 916 Tourist class seats.

1.  
FOLDOUT FRAME



-  Closet
-  Type A Doors
-  Galley (coffee, microwaves, etc.)
-  Galley (food, carts, etc.)
-  Laboratories
-  Air Office
-  Crew rest area

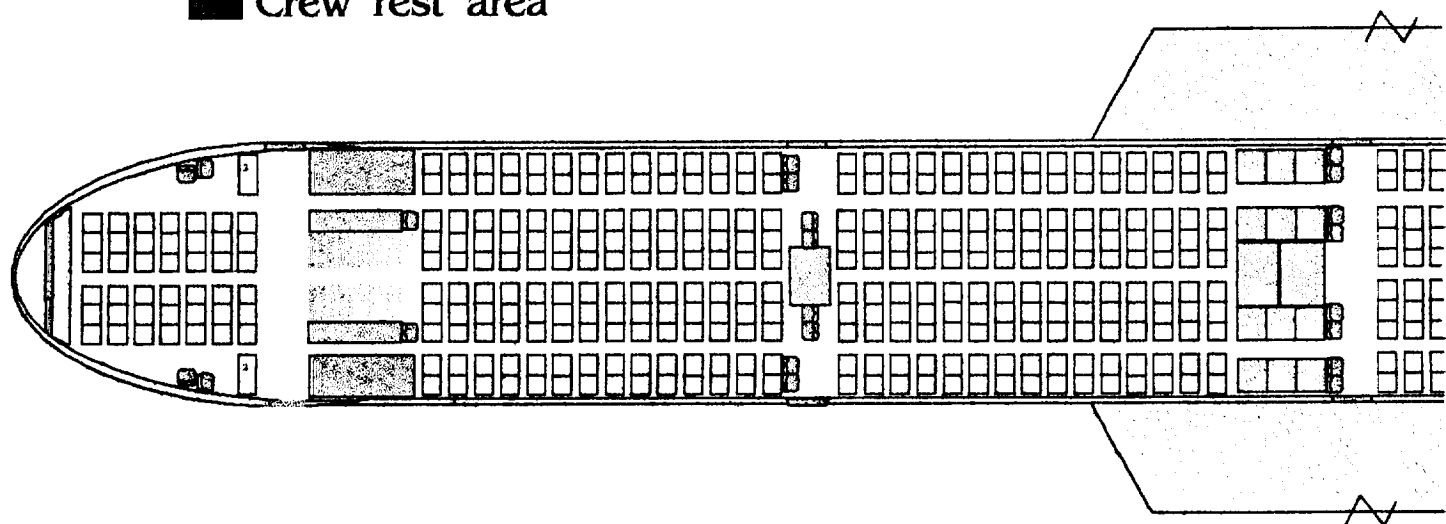
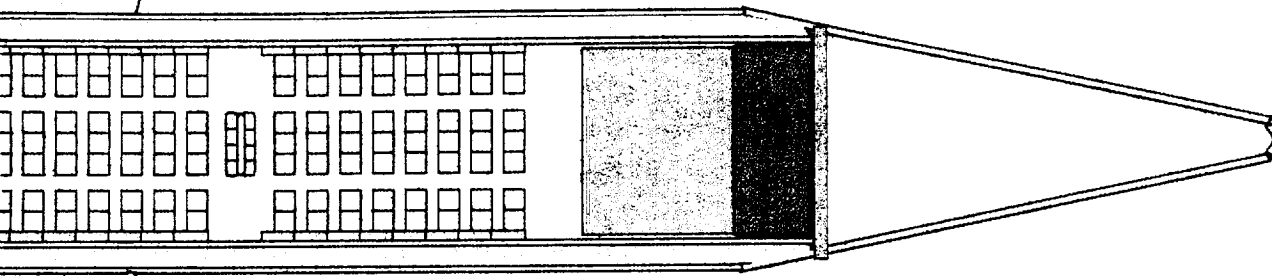


Figure 4. Interior Lay

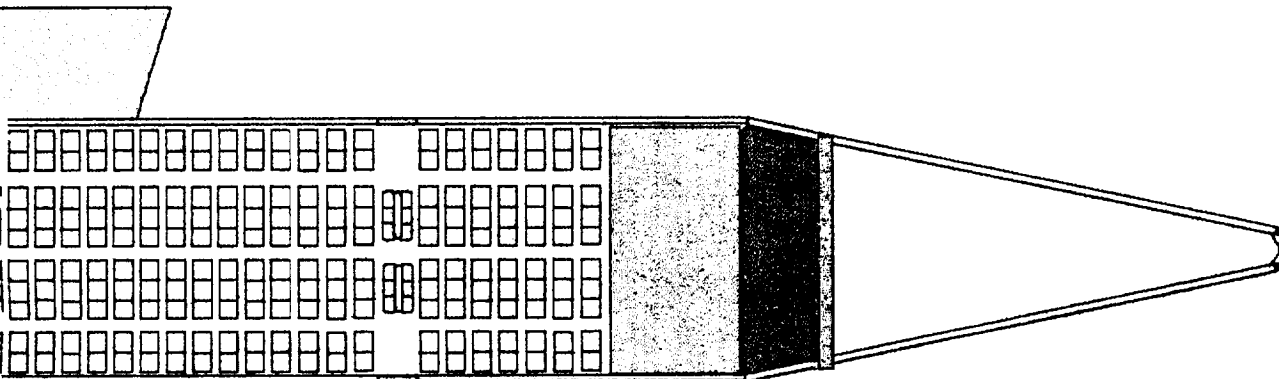
2

FOLDOUT FRAME



## Upper Deck

266 Business First  
PAX



## Main Deck

586 Business  
PAX

out

## 4.2. Passenger Safety

There are 16 Type A doors on the VLCT-13, allowing 1064 passengers to escape meeting FAR 36 requirements. The exits are spaced approximately 50 ft apart, Figure 1, providing easy access. Slides are located at each exit. The main deck slide are 17 ft from the ground at a  $35^\circ$  down angle. Figure 5.

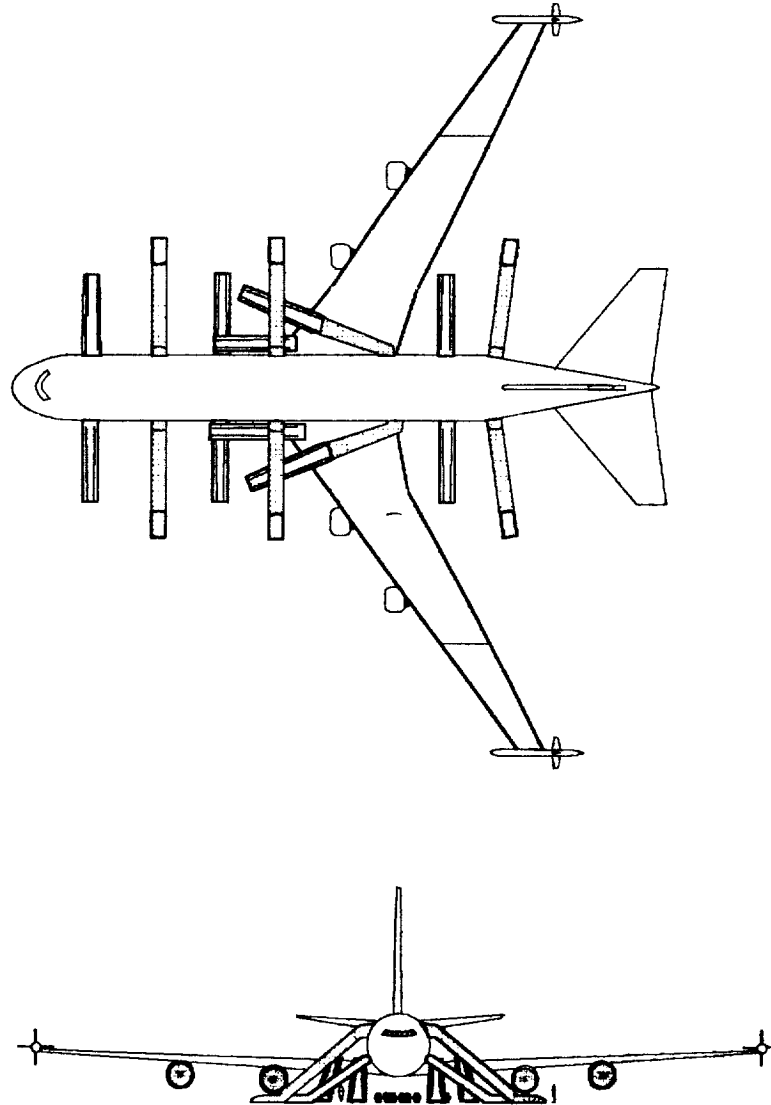


Figure 5. Emergency Egress

As can you see, the upper deck slides are very high, 27 ft. The down angle for this slide is  $40^\circ$ . The B747 has a  $40^\circ$  down angle from the upper deck.<sup>12</sup> These slides are tubes to prevent passengers from falling off

the slide and so they will not hold up egress because they are afraid of heights; out of sight out of mind. The slide is conventional on the ground.

#### 4.3. Cargo Section

Optimum use of the cargo deck involves using LD-3 containers. Calculating the weight of the baggage and multiplying by the volume capacity of an LD-3 container, 28 LD-3 containers will be required to carry all of the passenger baggage and 30,000 pounds of cargo. As seen in Figure 6, all of the cargo fits nicely in forward of the wing and aft of the nose gear. The length of the cargo section is 84 ft; the width is 15 ft. The lower deck also contains the avionics, air-conditioning, water and waste storage, as shown in Figure 6 below. The avionics is located forward of the nose gear. Six air-conditioning units are being used to supply the cabin with 20 ft<sup>3</sup>/min air movement. Three units are in the forward cargo section while the other three are aft of the main landing gear. Waste water and drinking water are located on either side of the cargo hold in the small section next to the skin while two larger tanks of each type of water is located aft of the landing gear. The lavs are located above the wing so this location helps in transportation of each type of water. There isn't much distance from the lavs to the tanks which means less space to look at in case there is a leak.

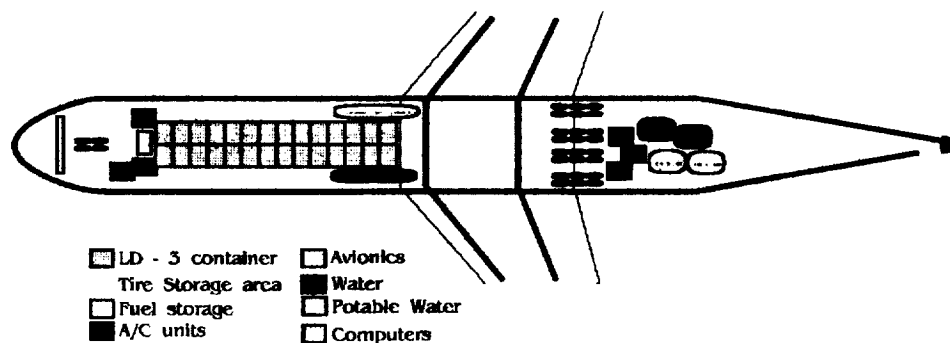


Figure 6. Cargo Hold

#### 4.4. Lavatories & Galleys

The number of laboratories was decided upon for the growth case of 1000 PAX. There is a lav for every 50 people which is average for most commercial airliners. There are 21 lavatories of approximately 4 ft x 4ft. The lavs are grouped so that they are far away from the galleys. Since this airplane will be sold on the



international market, many countries favor having the bathrooms far away from the food preparation area: a grouped arrangement facilitates cleaning after flight. As seen in figure 7, the main deck lavs with two air offices between the lavs.<sup>12</sup> The lavs open toward each other while the air office entrance is along the center aisle. Flight attendant seats for take-off and landing are placed on the lav wall. Two flight attendants can sit here for a total of eight.

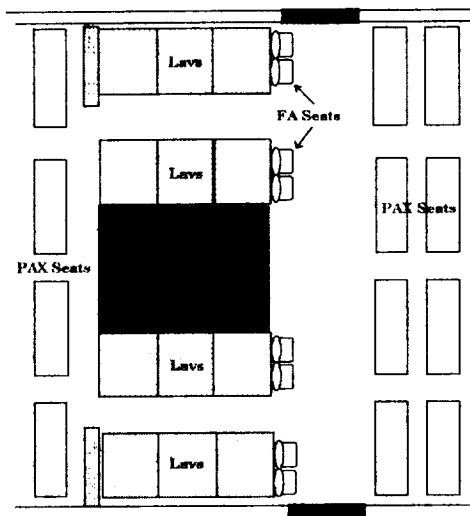


Figure 7. Lavatory Layout

The main deck lav layout was used as an example; examination of Figure 4 will show that the lavs on the upper deck are directly above the main deck lavs. This arrangement facilitates cleaning and plumbing maintenance.

Flight attendant seats are located all around the airplane. The attendants can watch everyone per FAR regulations. The island seats in the open space between emergency exits can be used in flight for passengers who want a change of scenery. A stroll to the lavs is actually no more than 130 ft. During a 16 hr flight, strolling space is an important passenger comfort. The center isle on the main deck facilitates movement by passengers around food cart blocking the outer isle's.

#### 4.5. Air Office

As business information is increasingly shared through the use of computers and phones, a business traveler will require an office with easy, quick access to these machines. An international business person will require this access to better utilize that flight time. On a 16 hour Pacific Rim flight, half of that time can now be used as part of the business day. An air office equipped with a computer, access to power for a laptop, air-to-ground phone, satellite hookup, fax, etc. will be available. A typical layout is shown in Figure 8.

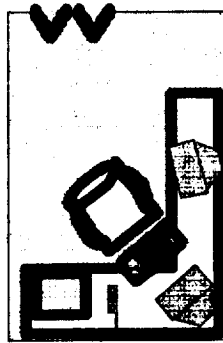


Figure 8. Air Office Layout

An air office could be transformed into an exercise room if an airline wished to offer such an arrangement. Two offices could be replaced with a conference room. An air office could also be changed into a children area, soundproofed with entertaining activities. The extra space available on a large airplane could bring back the early days of long haul flights, when there were sleeping areas, couches and bars.

## 5. COST ANALYSIS

### 5.1. Operating Cost

The Direct Operating Cost (DOC) per nautical mile, which includes flying, maintenance, depreciation and landing fees, is \$170 /nm. DOC is directly related to how well the airplane was designed. 500,000 total annual miles are flown with an annual utilization of 2000 hrs. DOC of maintenance constituted the highest cost to operators, \$57/nm. Labor cost on the engines alone was \$27/nm! A comparison of all maintenance costs are shown in Figure 9.

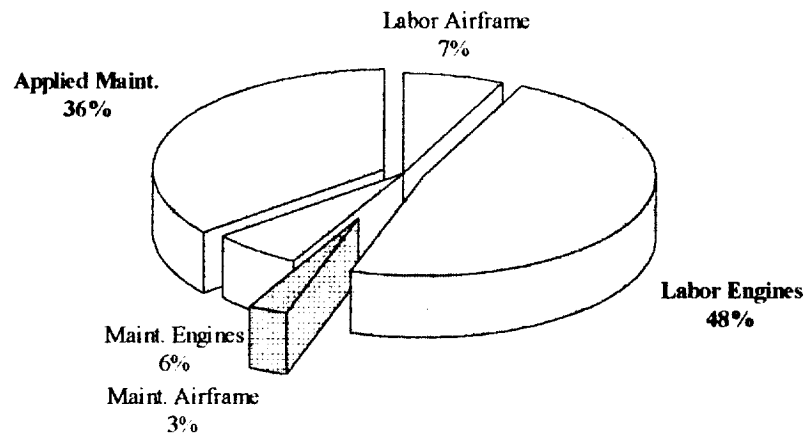


Figure 9. Distribution of Labor and Maintenance Costs

The DOC/PAX-seat mile for the 814 PAX configuration is 2.8 cents. As passenger loading increases, the DOC/PAX-seat mile decreases. For the growth version of 1012 PAX, the cost is 2.3 cents. Current aircraft are operating at a cost above 3 cents DOC/PAX-seat mile.<sup>11</sup>

Indirect operating costs were calculated by assuming that this cost was about 53% of DOC. {book 8} This was done because there is no exact method for calculating each cost included in the Indirect Operating Cost (IOC); not all airlines handle their operations the same. Based on an extrapolation from Figure 5.12 in Reference {book 8}, the 53% was used in the calculation for IOC. Items included in IOC calculations are:

passenger service, ground facilities, promotion, sales, entertainment, general administrative services and more. IOC costs are very hard for a designer to control because the airline decides how much to spend on these services.

## 5.2. Research and Acquisition Cost

Research, development, test and evaluation (RDTE) "lock in" 95% of the life cycle cost of the airplane. In all, the cost for RDTE segment is the lowest, Figure 10, but the decisions made are the most important. Decisions in this phase design the airplane. Changes in latter phases of the design process can not affect the cost of the airplane. At the end of this stage, the airplane is an airplane; the airframer has dedicated itself.

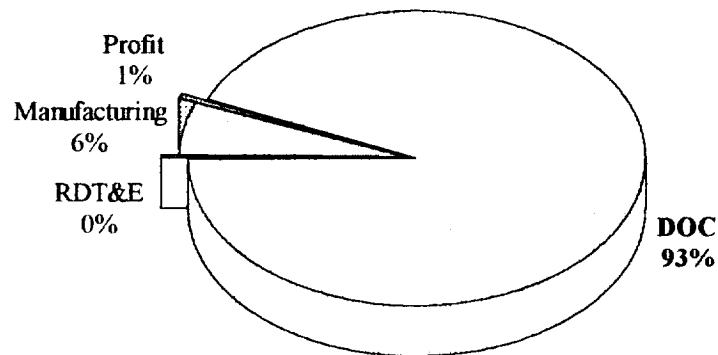


Figure 10. Breakdown of Life Cycle Costs

Manufacturing and acquisition constitute the next largest cost for an airplane program. Production costs including interior, labor, material and quality control contribute a large amount to this cost. The man-hours involved are on the order of  $10^8$  hrs!

### 5.3. Life Cycle Cost

Assuming 600 airplanes will be built to production standards an airplane market price of \$195 million dollars was calculated. This number compares well to the airplane estimated price of \$193 million dollars using the formula in reference 13. Assuming 600 airplanes would be produced was derived from Reference 2.

$$AMP_{1989} = \text{invlog}\{3.3191 + 0.8043\{\log(W_{to})\}\}$$

Using RDS Student, an airplane estimated price of \$227 million was calculated.<sup>14</sup> These similarities imply that the assumptions were good.

## **6. PRELIMINARY SIZING**

### **6.1. Weight Sizing**

Ascertaining the weight of the airplane was not determined by the configuration. Important parameters involved with the weight calculations were SFC of the engines, cruising speed, range, and intended cargo.

At first, traditional values of SFC and L/D were used, 0.5 and 18, respectively. It quickly became apparent that over 2 million pounds of airplane was not good. In order to lower the weight, the L/D was raised from 18 to 25, the SFC was lowered from 0.53 to 0.49. These values gave a take-off weight of 1.4 million pounds. The cruise speed was raised from 0.83 to 0.855 for a time because it was found that it also decreased our  $W_{TO}$ . This was later dismissed because the sizing program, from Reference 15, did not take into account the increase in drag, and it is very doubtful whether the engines could still run at the specified SFC.

To add a factor of safety to our plane, an additional range of 500 nautical miles was added to the cruising range. This is on top of the standard FAR requirements for fuel reserves and loiter conditions. This would give the plane more leeway if an engine isn't performing up to the SFC specified, or if there is more drag on the airplane than calculated theoretically.

### **6.2. Design Point**

The design point determines thrust, wing area and lift coefficient for takeoff and landing. The takeoff weight found in section 3.1 was used to determine thrust and wing area. The method of reference was used to construct the graph (Figure 11) to select the design point.

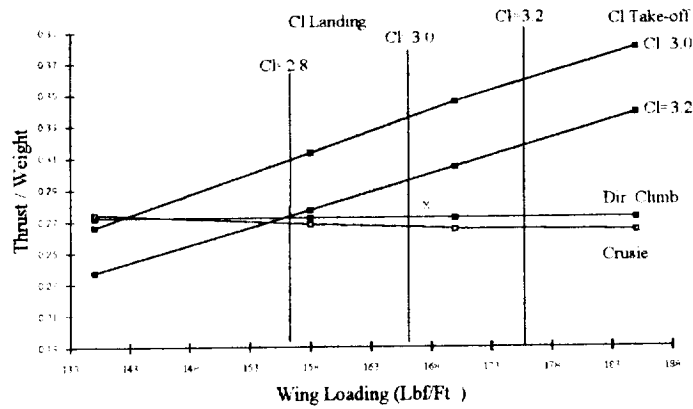


Figure 11. T/W vs. S/W

The initial sizing was calculated using the estimated values:  $L/D = 25$ ,  $e = 0.85$ ,  $AR = 10$ ,  $C_{Do} = 0.017$  and  $W_{TO} = 1.3$  million pounds. The VLCT-13 has to meet FAR 25 one engine inoperative takeoff climb requirements. Since the climb has the highest thrust to weight ratio, the requirement sets the thrust to weight at 0.26 (see Figure 11 ). The wing loading determines not only wing planform area and lift coefficient for takeoff and landing, but also takeoff and landing velocity. The VLCT-13 becomes much safer when takeoff and landing velocities are low, but the VLCT-13 spends most of the time at cruise. When the VLCT-13 operates at least thrust to weight ratio at cruise, the least amount of fuel is used for the travel. When the wing loading is  $155 \text{ lbf/ft}^2$ , the cruise curve shows the least thrust to weight ratio. This wing loading gives high takeoff velocity for the VLCT-13, but considering airline's operational cost for sales purpose, the wing loading of  $155 \text{ lbf/ft}^2$  thus the initial design point has a thrust to weight ratio of 0.26 and a wing loading of  $155 \text{ lbf/ft}^2$ . The final sizing was found by using calculated values of:  $L/D = 21$ ,  $e = 0.77$ ,  $AR = 11.63$ ,  $C_{Do} = 0.0166$  and  $W_{TO} = 1.4$  million lbm. The same analysis was followed to determine the final design point. Thrust to weight was increased to 0.28 because of the increment of weight and the lowest thrust to weight ratio at cruise occurs when the wing loading is at  $168 \text{ lbf/ft}^2$ . The values obtained from sizing graph showed table below.

Table 6-1 Design Point Summary

Wing area	8,000 $\text{ft}^2$
Required thrust at takeoff	392,000 lbf
Takeoff lift coefficient	3.2
Landing lift coefficient	3.1

## 7. WING DESIGN

The VLCT-13 spends most of its time (8-13 hrs) cruising at Mach 0.83. Consequently, its wing must be designed to maximize its performance in cruise. therefore, a subsonic wing is designed for the VLCT-13. The wing planform area of 8000 ft<sup>2</sup> was obtained from preliminary sizing.

A typical subsonic wing has a sweep angle to avoid compressibility effects. Sweep angle also affects lift distributions, drag, aerodynamic center and structural weight. For structure consideration, as the sweep angle is swept back beyond 35 degrees, the torsion induced by lift will increase significantly. Specifically, as the sweep angle is increased, the aerodynamic center gets pushed back increasing the distance from the aerodynamic center to the front spar. The increase torsion will have an effect of increasing the skin thickness at the root of the wing. Compressibility effect is important at the cruise Mach number of 0.83. When the local Mach number is close to one, it forms wave drag. The VLCT-13 has to have enough sweep angle to reduce the local Mach number. Local Mach number less 0.7 is necessary to avoid compressibility effect, therefore a sweep angle of 35° was implemented into the wing.

A high aspect ratio was selected for VLCT-13 because there are two advantages for the high aspect ratio. Induced drag factor is inversely proportional to aspect ratio, but aspect ratio has a much stronger effect on induced drag coefficient than the value of the induced drag factor; therefore, the high aspect ratio reduces overall drag. Another advantage for the high aspect ratio is one engine inoperative case. In low speed climbing or cruising, induced drag occupies the majority of the total drag. Since the high aspect ratio wing reduces overall drag, the induced drag would decrease. When the aspect ratio reached 11.6, the VLCT-13 obtained the highest L/D; therefore, the VLCT-13 has a high aspect ratio of 11.6, compared to that of the Boeing 747's aspect ratio of 7. The wingspan of 305 feet was calculated from the AR of 11.6 and the wing planform area of 8,000 ft<sup>2</sup>.

The root chord has to be strong enough to withstand structural weight of the wing as well as the aerodynamic forces on the wing. The VLCT-13 required a root chord of 50 ft. with a thickness of 6 ft. for structural reasons.



A wing with a low taper ratio is better, but not less than 0.2 because the tip stall tendency becomes excessive. A lower taper ratio has a higher lift coefficient on the outer portion of the wing as the downwash pattern changes to move the lift distribution toward the elliptical. This tends to encourage tip stall. A low taper ratio also reduces induced drag factor and leads to larger chords and physical wing thickness inboard, reducing the aerodynamic bending moment. Stability and control are affected by aerodynamic center that is function of taper ratio. A taper ratio of 0.2 was chosen to satisfy all parameters. Some wing dimensions are shown in Table7-1.

Table 7-1. Wing Information

Aspect Ratio	11.63
Span	305 ft.
Surface Area	8000 ft <sup>2</sup>
Sweep Angle	35 deg
Taper Ratio	0.20
Root Chord	50 ft.
Tip Chord	12.5 ft

## 7.1. Airfoil

The primary force that governed the airfoil selection was the required cruise Mach number of 0.83. It was essential to find an airfoil that had a critical Mach number at or around the cruise velocity. Originally, NACA airfoils were examined as possible candidates. However, it was determined that the drag rise with Mach number was insufficient. The next step was to examine Super Critical airfoils. The Super Critical airfoil (SCA) had three major advantages over the NACA airfoils. The first advantage was that the basic shape of the airfoil. The SCA has a larger cross sectional area than the NACA airfoils. Due to the aircraft's required range of 7000 nautical miles, the large wing cross sectional area allowed for a substantial fuel volume. An additional advantage of the airfoil shape was that it allowed for a strong torsional box to be built between the front and rear spar.

The second advantage was that the critical Mach number was close to the aircraft's cruise speed. With this information in mind, the CAST 10-2 with a 12 % thick airfoil with the maximum thickness at 40% chord. The maximum lift coefficient for this airfoil is 1.1 at an angle of attack of 8 degrees (Figure12).

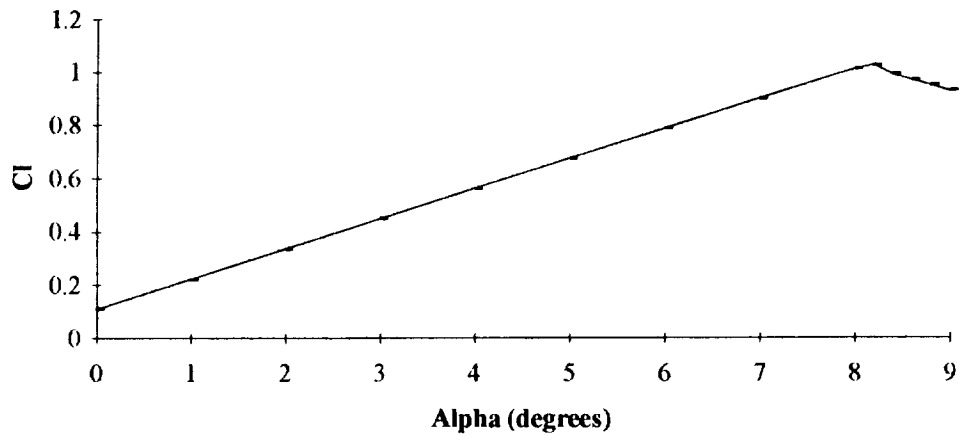


Figure 12. CAST 10-2 Section Lift Coefficient vs. Alpha

## 7.2. High Lift Devices

The VLCT-13 is equipped with leading edge and trailing edge devices to generate additional lift for take-off and landing, Figure 13.

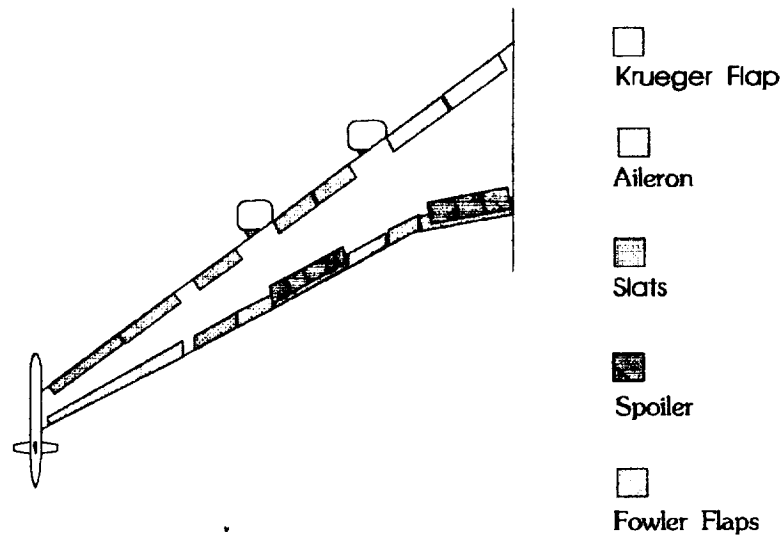


Figure 13. High Lift Devices

The single-slotted Fowler flap was chosen as the trailing edge device because in comparison with other trailing edge devices, the Fowler flap generates the most lift and least drag. As an example, Table 7-2 compares the increase in lift and corresponding drag penalty of four types of flaps at a deflection of  $20^\circ$ .

Table 7-2. Flap Comparisons

Flap Type	$\Delta C_L$	$\Delta C_{dP}$
Split	0.60	0.025
Plain	0.63	0.037
Single-Slotted	0.90	0.018
Fowler	1.48	0.037

As shown above, the highest parasite drag increase is associated with the Fowler flap and plain flap. The increase in lift associated with the Fowler flap outweighs the drag penalty. The disadvantage of using Fowler flaps is the increased weight; the track system is made of steel. To compensate, the flaps will be composed of graphite-epoxy, comprising a 5% weight savings as compared to making the flaps out of aluminum.

The leading edge of the wing is equipped with variable cambered Krueger flaps and slats. These are cambered because the slats can be adjusted so that the leading edge allows for incoming airflow to remain attached. Variable cambered Krueger flaps are more efficient in delaying stall than fixed cambered flaps. The Krueger flaps and slats were sized based on the location of the front wing spar located at 17% chord. Each flap and slat section is 6.9 ft long. The chord is 13% of the wing chord. Two sections of Krueger flap are placed inboard, next to the fuselage. Krueger slats are located on the outboard sections of the leading edge, Figure 13. The reason for the combination of flaps and slats is positive longitudinal stability, pitch down, during stall. The inboard portion of the wing will stall first contributing to a pitch down attitude; the major portion of lift is not lost by the entire wing stalling!

The maximum lift coefficient achieved by the wing at take-off and landing is 0.925. To increase the overall lift coefficient to 2.8 during take-off, the flaps are deflected  $32^\circ$ . This flap deflection increases total  $C_{L,max}$  by 2.0. At landing, flap deflection is  $40^\circ$  to attain a lift coefficient of 2.95. At these deflections, a significant amount of noise is generated, but meets Stage 3 noise requirements.

Included aft of the inner engine, is an inboard aileron utilized during cruise. Another aileron is located outboard for use in low speed maneuvering. Referring to Figure 13 above, the trailing edge is dominated by Fowler flaps. To avoid intruding upon the wing box, the flaps are sized so the width ranges from 75% to 100% chord. The rear wing spar is located at 70% chord. Spoilers along the trailing edge at the mid and inboard wing sections, utilized during high speed maneuvering and assisting in braking at landing.

The mid spoilers will aid the inboard aileron during roll maneuvers. The spoilers width is 71% to 77% chord.

## 8. EMPENNAGE DESIGN

### 8.1. Configuration

Two empennage configurations were investigated for possible use on the VLCT-13. These possibilities included a V-tail, discussed in section 3, and a conventional tail. An additional argument for a conventional empennage design was the aircraft's fuselage shape, circular. The VLCT-13 would experience additional interference drag with a V-tail design.

The conventional tail configuration was decided upon because of interference drag savings, weight savings and reduced manufacturing complexity. Stability and control problems were also reduced.

### 8.2. Planform Parameters

The geometry of the empennage is outlined in Table 8-1. The preliminary sizing of the horizontal tail was accomplished by comparing the area of the surface with other similar, smaller aircraft, i.e. B-747, MD-11, MD-12. The empennage was initially designed following the guidelines in reference 15. After stability and control analysis was done, the horizontal tail has the dimensions in Figure 14a, while the vertical tail is dimensioned in Figure 14b.

Table 8-1. Empennage Data

	Vertical Tail	Horizontal Tail
Aspect Ratio	1.8	3.7
Span	55 ft.	98 ft.
Surface Area	1700 ft <sup>2</sup>	2600 ft <sup>2</sup>
Sweep Angle, $\frac{\pi}{4}$	38 deg	34 deg
Taper Ratio	0.32	0.30
Root Chord	48 ft.	37 ft.
Tip Chord	15 ft	16 ft

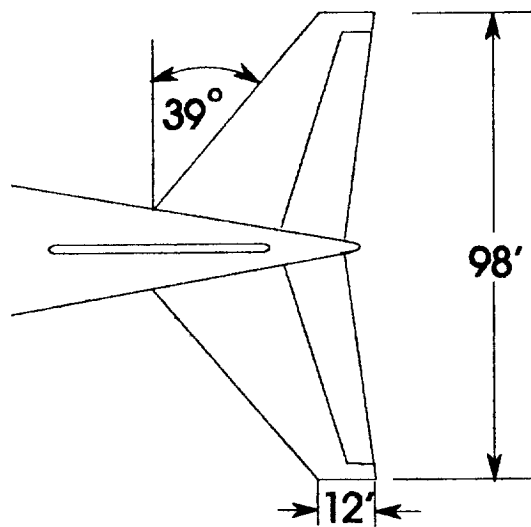


Figure 14a. Horizontal Tail

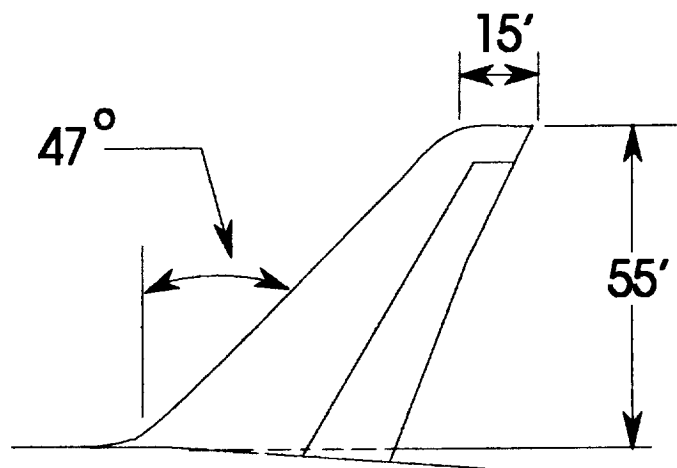


Figure 14b. Vertical Tail

### 8.3. Airfoil Selection

The horizontal tail airfoil selection was driven primarily by the main wing stall characteristics. In order to ensure reasonable stall recovery, the horizontal tail must stall well after the main wing. This is why the NACA 0016 airfoil section was chosen. The NACA 0016 airfoil section stalls at three degrees angle of attack above the stall angle of the main wing.

#### 8.4. Drag Polar

In order to construct the design point and to determine the performance of the VLCT-13, the drag polar was one of the parameter that effects on the performance. The drag polar was calculated for takeoff, landing, climb, cruise at 36000 ft and at 40000 ft.

The wetted area, lift coefficient, aspect ratio and airplane efficiency factor were necessary to compute the drag polar. The takeoff and lift coefficients were obtained from the design point. The airplane efficiency factor was calculated using reference 16. The wetted area was calculated for all the portions using references 16 and 17. Table 8-2 shows the values necessary to compute drag polar and Table 8-3 shows wetted area of each portion.

Table 8-2. Characteristics of VLCT-13.

Takeoff lift coefficient	3.2
Landing lift coefficient	3.1
Aspect ratio	11.63
Airplane efficiency factor	0.77
Lift coefficient at 36000 ft	0.80
Lift coefficient at 40000 ft	0.70

Table 8-3. Wetted area of VLCT-13.

Wing	14,000 ft <sup>2</sup>
Fuselage	19,000 ft <sup>2</sup>
Vertical tail	2100 ft <sup>2</sup>
Horizontal tail	4700 ft <sup>2</sup>
Engines	1850 ft <sup>2</sup>

The drag polar was operated using references 16 and 17. The average weight 1.3 million lbm for cruise at 36000 ft and 1.14 million lbm for cruise at 40000 ft were used to calculate the lift to drag ratio. The table below shows the lift to drag values obtained for drag polar.

Table 8-4. Lift to drag ratio for each phase.

Phase	L/D
Take off	7.5
Climb	19.5
36 k Cruise	21
40 k Cruise	21
Landing	8.4

## 9. PROPULSION SYSTEM

### 9.1. Engines

A thrust of approximately 400,000 lbf is required to get the VLCT-13 off the ground. Engines at this thrust level are currently in development and testing. Rolls-Royce is confident that their Trent 800 family will attain 100,000 lbf of thrust by the end of the century.<sup>18</sup> Pratt & Whitney are also developing an engine in this category; increasing the thrust of the PW 8084. General Electric is currently testing the GE 90. A static thrust level of 105,400 lbf was attained on during a 45 min test on April 3, 1993.<sup>19</sup>

### 9.2. Thrust Required

Most of the VLCT-13's mission is spent in cruise. Initially, a cruise altitude of 40,000 ft was desired; drag reduction. According to Figure 15, flying at 40,000 ft was impossible.

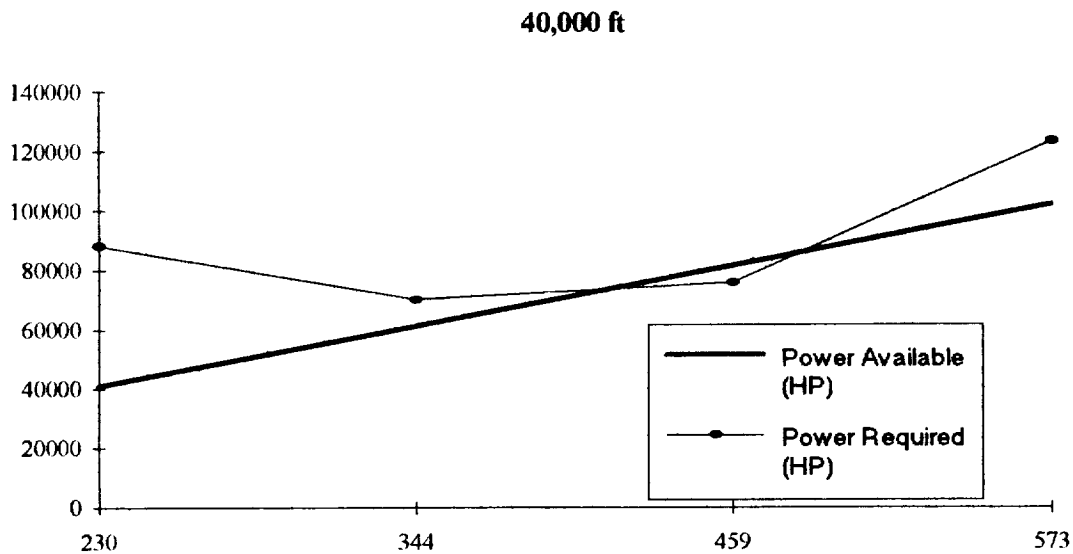


Figure 15. Power Operation for 40,000 feet

The envelope between thrust required and thrust available was small.



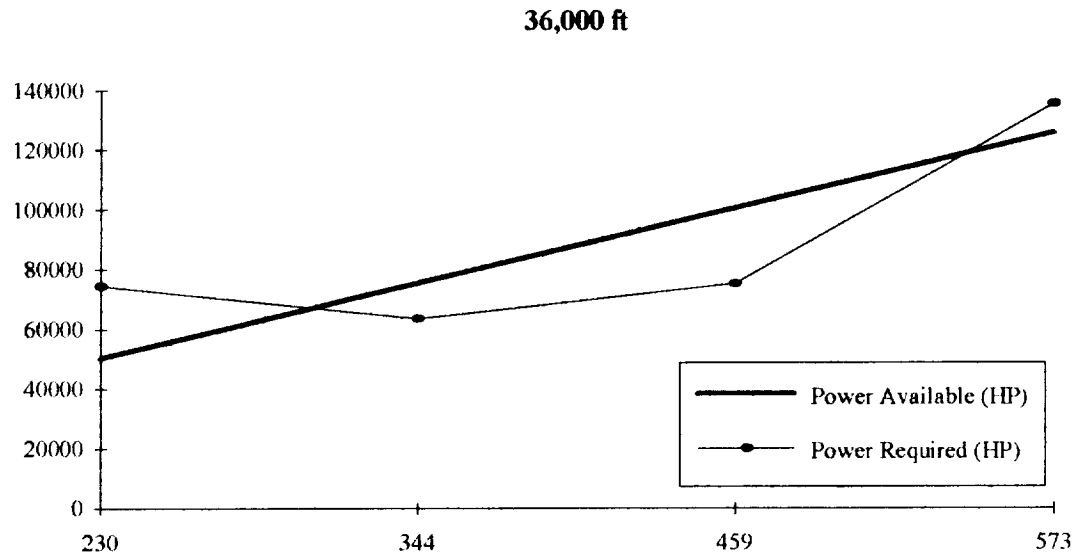


Figure 16. Power Operation for 36,000 feet

The VLCT-13 performs a step climb from an initial cruise at 36,000 ft to take advantage of the drag reduction. This initial cruise segment is required to burn some fuel. Figure 16 shows the operating section for the VLCT-13 at 36,000 ft. There is a large space between the thrust available and the thrust required. Good operation range.

### 9.3. Vortex Turbine

To get the SFC required for the engines, bleeding must be kept to a minimum. To help get the required energy for the airplane's electrical, hydraulic and laminar flow control systems, a vortex turbine was mounted on each wing tip. A vortex turbine is a device that captures the energy from a wing tip vortex with its turbine blades, which will be cambered and tapered to maximize efficiency. Figure 17 below.<sup>20</sup> From model tests of the turbine, it is expected that the power output from the turbine could reach 400 horsepower per wing tip. This is enough to power an aircraft with all electrical systems and a boundary layer control system.

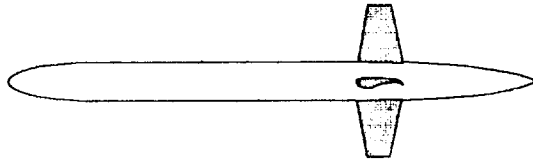


Figure 17. Vortex Turbine

The vortex turbine also has the side benefit of reducing induced drag on the wing. Since induced drag is 35% to 40% of the total cruise drag, this was considered to be a major side benefit. The only additional drag occurs when there is no lift on the wing. If there is no lift, there are no wing tip vortices, the turbine blades will not turn, so there will be increased drag due to the wetted area and skin friction of the turbine.

## 10. PERFORMANCE

### 10.1. Takeoff

While meeting the FAR takeoff requirement and clearing a 35 ft. obstacle, the VLCT-13 uses 6600 ft. of runway. The takeoff lift coefficient of 3.2 and wing area of 8,000 ft<sup>2</sup> from the preliminary sizing were used to calculate the critical velocity (125 knots). Using a 20% safety margin, the takeoff velocity of 150 knots was calculated. The average velocity during takeoff is 105 knots and ground roll distance 5980 feet was calculate by method in reference 21. therefore, the time required to takeoff is 34 seconds; and the average acceleration is 7.55 ft/s<sup>2</sup>. The VLCT-13 can produce enough excess thrust to meet the requirement above. The minimum flight path angle of 3.3 ° is required to satisfy the FAR 25 takeoff requirements.

### 10.2. Climb

As the RFP requirement, the aircraft has to climb to 36,000 ft within 25 minutes. Table 10-1 shows how VLCT-13 meets the requirement. The VLCT-13 accelerates from takeoff to 25,000 ft and maintains a constant velocity, 444 knots, thereafter to 36,000 feet. The VLCT-13 can not climb directly to 40,000 ft. because the engines do not produce the excess thrust needed. After cruising at 36,000 feet for 2 hours and 30 minutes the VLCT-13 climbs to 40,000 ft. within 10 minutes.

Table 10-1. Climb Performance

Altitude (ft)	Angle (deg)	Velocity (knots)	RoC (ft/s)
Sea Level to 5,000	4.7	237	27.8
10,000	5.6	250	40.0
15,000	3.5	326	29.6
20,000	2.7	385	28.2
25,000	1.9	444	23.2
30,000	1.9	444	24.8
36,000	1.1	444	14.4

### 10.3. Cruise

Because of the VLCT's large weight, the VLCT-13 has to fly about 2 hours and 20 minutes at an altitude of 36,000 feet. The aircraft can not actually attain an altitude of 40,000 ft. until some fuel has been

burned off. After this time, the aircraft can climb to 40,000 ft. within 10 minutes. The reason for cruising at 40,000 ft. is in terms of fuel consumption. The engine's specific fuel consumption at 40,000 ft. is lower than at 36,000 feet. while the SFC stays the same between 40,000 and 45,000 feet based on PW 4084 engine chart. The aircraft flies above 40,000 ft is better for the VLCT-13 in terms of fuel consumption. Average cruise time is expected to be about 8-12 hr's. If the VLCT-13 can fly at 40,000 ft. for most of this, fuel will be saved.

Cruising at an even higher altitude was studied because of the SFC savings. If the aircraft did try to fly at an altitude approaching 45,000 ft. the increased induced drag force due to lower density. The cruise Mach number for both altitudes is 0.83. A study was performed to fly faster,  $M = 0.85$ , which would decrease flying time by 17 minutes, but an extra 6000 lbm of fuel would have to be carried in the airplane. Besides, after 8 hr's, who will be able to tell that the flight was 17 minutes shorter? The cruise Mach number is faster than current Boeing 747's,  $M = 0.79$ .

#### 10.4. Descent

The aircraft starts to descend about 140 nm from the airport, keeping a constant descent angle of  $2.5^\circ$ . The aircraft would loiter at 10,000 ft, velocity of 177.7 knots if it is necessary. Refer to Figure 2 in section Mission Description.

Table 10-2. Descent Data

Altitude (ft)	Angle (deg)	Velocity (knots)	RoC (ft/s)
35,000	-2.5	414.7	32.7
30,000	-2.5	355.5	28.3
25,000	-2.5	296.2	24.0
20,000	-2.5	237	19.6
15,000	-2.5	207.4	16.3
10,000	-2.5	177.7	14.1
5,000	2	148.1	9.6
touch down	2	145.2	0.0

For descent to landing, after loitering, the aircraft maintains a 2 deg descent angle from 10,000 ft until landing and flare. These numbers are shown in the above table.

## 10.5. Landing

To meet FAR 25 landing requirement, the VLCT-13 must land within landing field length of 6,600 feet. The landing weight will be approximately 70% of the takeoff weight for a 7,000 nm range. The landing  $C_L$  3.1 is obtained from the design point and the approach velocity is calculated to 145.2 knots. The critical velocity is 112.6 knots, giving a 30% safety margin between approach and critical velocities. The aircraft maintains constant velocity from the 50 ft point until touch down. The VLCT-13 has the ability to stop within 5,170 ft without using thrust reverses.

## 10.6. Performance Summary

Table 10-3 is a summary of flying time and distance for a typical mission. Also shown is fuel burn for each segment.

Table10-3. Performance Summary

Segment	Time (hr.)	Distance (nm)	Fuel (lbm)
Take-off	0.009	1.1	6,300
Climb - 1	0.41	141	26,000
Cruise - 2	2.11	1050	69,000
Climb - 2	0.16	94	5,800
Cruise - 2	11.76	5580	310,000
Descent	0.57	137	11,000
Loiter	0.5	0	9,700
Landing	0.009	1.1	7,400

## **11. STABILITY AND CONTROL**

A preliminary stability and control analysis of the VLCT-13 was performed considering both static and dynamic stability. Two flight conditions were of specific interest: 1) approach flight dynamics below Mach 0.2 and 2) cruise at 40,000 feet at Mach 0.83. Utilizing Digital DATCOM for the determination stability derivatives, the aircraft's short period frequency ( $\omega_{sp}$ ) and the short period damping ( $\zeta_{sp}$ ) were determined.<sup>22</sup> From these derivative, the VLCT-13 rated Level 1 for the approach task and Level 2 for the cruise task. This level rating is outlined in MIL-STD 1797A. A Level 1 rating on the aircraft indicates that the handling qualities of this aircraft are superior. A Level 2 rating indicates that the aircraft would be capable of performing the task, but the pilot had to do some work.

### **11.1. Static Margin Assessment**

A longitudinal x-plot, shown in Figure 18, was generated using the initial method of Reference {book2}. From this analysis, the preliminary sizing of the vertical tail was performed. It was decided that the aircraft should be inherently stable due to the size and the mission of the aircraft.

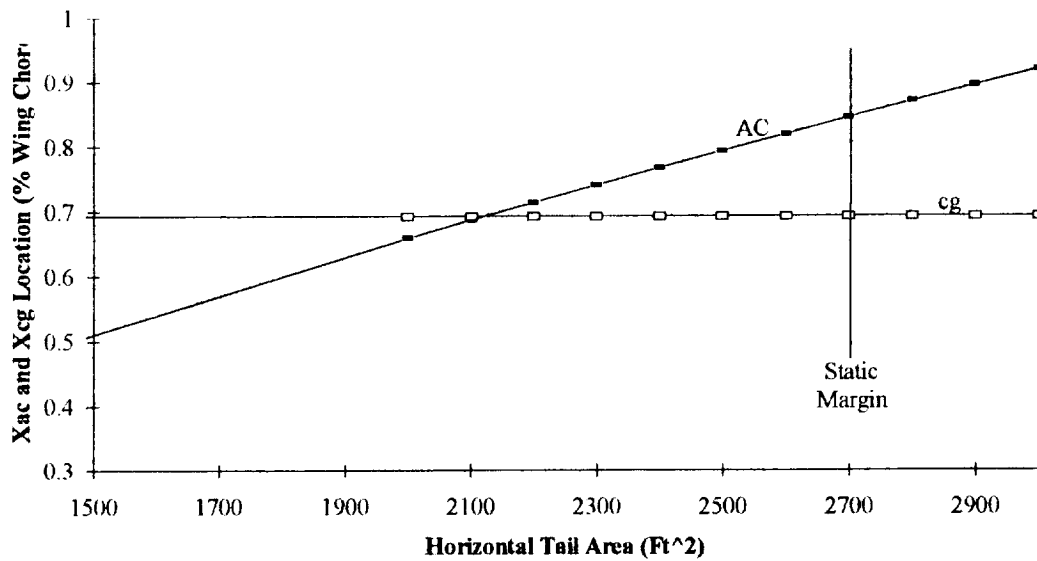


Figure 18. Longitudinal X-plot

From the Longitudinal X-Plot, a static margin of fifteen percent was chosen by the suggestion of Reference 23. With the static margin chosen, the aircraft can achieve rotation and sufficient maneuvering qualities.

## 11.2. Static Stability Assessment

The static stability derivatives of the VLCT-13 were generated for two flight conditions outlined in Table 11-1 using output generated using Digital DATCOM.<sup>22</sup>

Table 11-1. Flight Conditions for Stability Analysis

	Approach Conditions	Cruise Conditions
Mach No.	0.2	0.83
Altitude	5000 ft.	40,000 ft.
Configuration	Fully Loaded	Fully Loaded
Static Margin	15 %	15 %
Weight	1.4 million lbs	1.4 million lbs
Ixx	$1.4 \times 10^8$ slugs-ft <sup>2</sup>	$1.4 \times 10^8$ slugs-ft <sup>2</sup>
Iyy	$1.1 \times 10^8$ slugs-ft <sup>2</sup>	$1.1 \times 10^8$ slugs-ft <sup>2</sup>
Izz	$3.6 \times 10^8$ slugs-ft <sup>2</sup>	$3.6 \times 10^8$ slugs-ft <sup>2</sup>

Using the static stability derivatives calculated with the information in Table 11-1, it was possible to generate the dynamic stability derivatives.

Table 11-2. Stability Derivatives

Stability Derivative	Approach Condition	Cruise Condition
$C_{L\alpha}$ (1/rad)	5.660	5.296
$C_{m\alpha}$ (1/rad)	-8.078	-7.792
$C_{y\beta}$ (1/rad)	-0.546	-0.555
$C_{n\beta}$ (1/rad)	-0.095	-0.089
$C_{l\beta}$ (1/rad)	-0.137	-0.142
$C_{lq}$	34.320	33.804
$C_{mq}$	-48.873	-48.082
$C_{l\dot{\alpha}}$	6.772	6.497
$C_{m\dot{\alpha}}$	-12.405	-14.094
$C_{lp}$	-0.382	-0.350
$C_{yp}$	0.023	0.017
$C_{np}$	-0.096	-0.090
$C_{nr}$	-0.011	-0.006
$C_{lr}$	0.182	0.182

A summary of these derivative are outlined in Table 11-2 above. From this information, the stability short period frequency and damping coefficient were developed for each flight condition. Based on a Category B aircraft (Category B - Aircraft requiring only gradual maneuvers without precision tracking), both the frequency and the damping coefficient indicated that the aircraft rated Level 1 for the approach task. In addition, the aircraft rated Level 2 for the cruise task (Table 11-3). The difference between the two ratings was based on the decrease in value of the damping coefficient at higher Mach numbers. By implementing a stability augmentation system for additional longitudinal control, the damping in the short period could be increased. This would result in a Level 1 aircraft for the overall mission and yield a smoother ride in cruise.

Table 11-3. Longitudinal Handling Qualities Assessment

Flight Condition	Short Period Damping ( $\zeta_{sp}$ )	Rating
Approach	0.300	Level 1
Cruise	0.288	Level 2



## 12. STRUCTURES

### 12.1. Materials

Since the VLCT-13 will be cruising at a subsonic speed of  $M = 0.83$ , aircraft skin temperature is not a factor in structural design. Typically, an aluminum alloy loses strength when an aircraft surpasses  $M = 2.0$  because of temperature at this Mach range would surpass the aluminum temperature limit of  $350^{\circ}\text{F}$ . The highest temperature seen by the VLCT-13 will be at the nose, on the leading edges and over the top of the wings. The temperature at these areas are not expected to surpass  $250^{\circ}\text{F}$ .

With this in mind, the priority at this point would be to accommodate the structural requirements imposed by aerodynamic and inertial loads at the lowest possible cost and weight penalty. Considering the above restrictions, it seemed that Aluminum-Lithium (Al-Li) was the material to use because of its low cost, high strength and for its superior fatigue resistance. Compared to conventional aluminum alloys, e.g. 2024-T3 and other T-series alloys, Al-Li is 10% lighter and stiffer. Aluminum-Lithium also has excellent fatigue performance.<sup>24</sup> The Al-Li makes up 80% of the exterior material that covers the VLCT-13.

According to Reference 4 those airframers studying building an aircraft of this size are considering using Aluminum-Lithium in their design. There are advantages and disadvantages to using this material are listed in Table 12-1.

Table 12-1. Al-Li Advantages/Disadvantages

Advantages	Disadvantages
manufacturers can use existing machinery & equipment to work material	higher costs than regular aluminum, 3X, but lower than titanium or composites
workers require no special training, reducing production costs	safety precautions in casting
superior fatigue resistance	need for closer control of processing parameters
lighter weight	
greater corrosion resistance	
10% greater tensile strength	

Since this material is very workable, methods used to prevent corrosion on regular aluminum alloys may also be applied to Aluminum-Lithium. Such surface treatments are aluminum cladding, surface conversion treatments and organic protective coatings. These are standard corrosion prevention methods currently being applied on soft metals such as aluminum; therefore, would not increase total costs significantly.

For flaps, ailerons, elevators and all high-lift devices, composite material, graphite-epoxy, will be used. Graphite-epoxy will also be used to cover the folding wing section because of its low weight density ( $0.056 \text{ lbm/in}^3$ ) and high tensile strength of 170 ksi. The low weight density reduces the weight of the section by 75%, lowering the overall wing weight by 8%. This reduction in the section weight is hoped to decrease fatigue and maintenance costs for the hinge connecting the folding section to the main wing.

For the interior structure, the VLCT-13 will utilize the high strength of Steel H-II. This material will readily and easily carry the interior loads due to cargo and passengers.

Extensive application of composites for the VLCT-13 was rejected because of high acquisition costs, need for higher-skilled labor and start-up production costs. Another large factor in not utilizing composites more is the technology unknowns.

## **12.2. V-N Diagram**

The V-n diagrams features the maneuver envelope which sets the structural limits and the gust envelope which shows the loads imposed on the aircraft from the atmospheric disturbances. The VLCT-13 for the most part is maneuver-critical but when the cruise equivalent airspeed reaches 400 ft/s, the aircraft becomes gust-load sensitive as well.

The maximum positive load factor is 2.5. This limit was calculated based on FAR-25 requirements. The maximum dive speed is 500 ft/s; therefore, structural damage will occur if the lift force is 2.5 times that of the airplane gross weight or if the equivalent airspeed exceeds 500 ft/s. To maneuver effectively, the speed of the aircraft should be 240 ft/s. Furthermore, to prevent stall, the VLCT-13 should not fly slower than 148 ft/s EAS.

### **12.2.1. Wing**

The wing is used as a load carrying structure for fuel, engines, high-lift devices and aerodynamic loading. Because of the very large span (305 ft.) of the VLCT-13, the wing was split into two sections for airport compatibility (Figure 20). The main wing section and a 50ft. folding section.

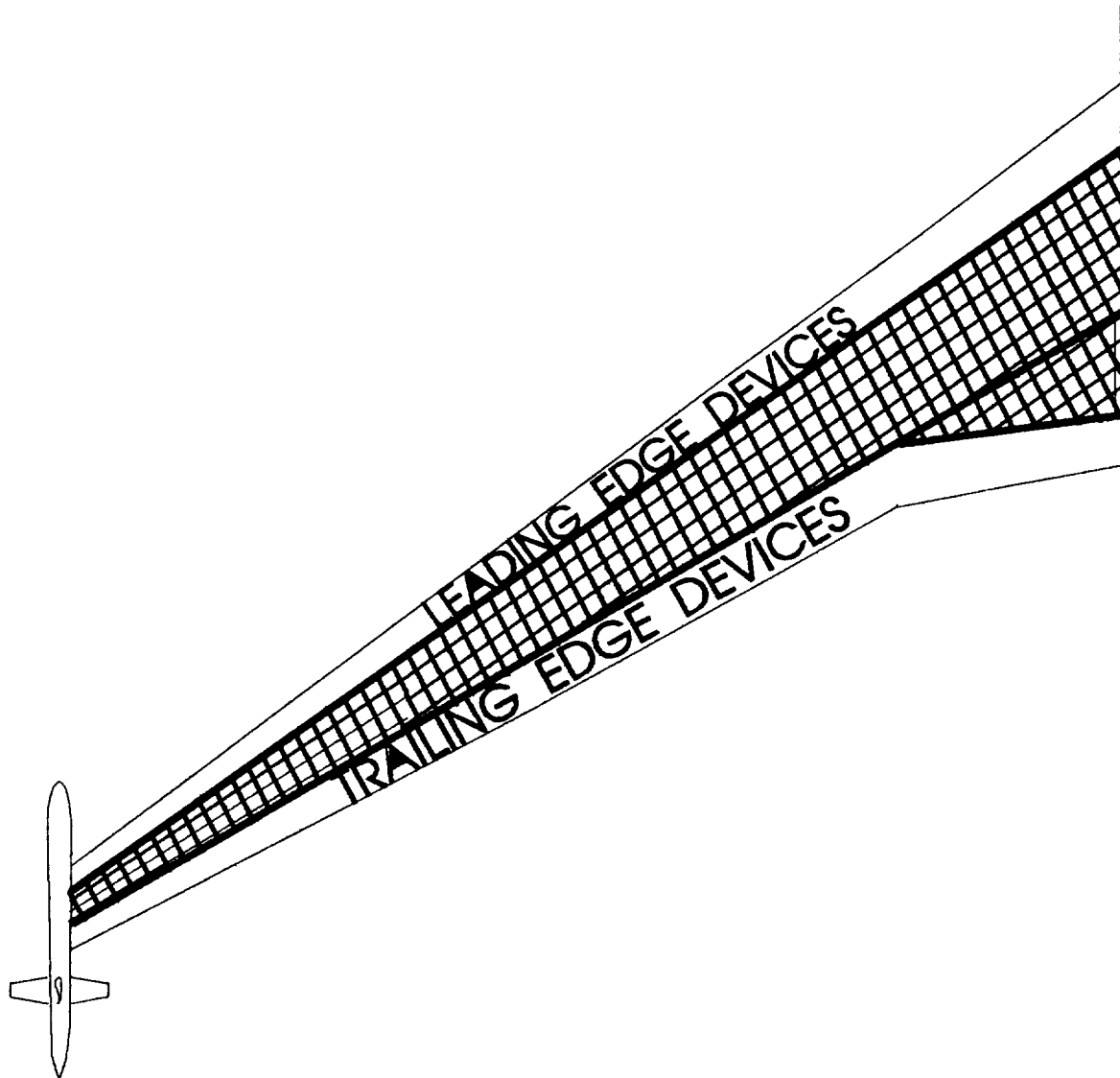


Figure 20. Structure of Wing

The location of critical importance in the wing is the root. This location experiences the highest bending moments and the highest normal and shear stresses. The wing-box components analyzed for shear

and bending loads are the following: spars, skin, stringers, and ribs. The dimensions of a component and material used are sized according to structural requirements. For any wing-box structure, the applied load must be less than the material allowable load utilizing a factor of safety of 1.5.

The applied loads are a function of design. These loads can be reduced by increasing the moment of inertia of the structure or by decreasing the applied loads. The weight density of a material is an important factor to consider when choosing a material.

Because of the high sweep of the wing, the skin must be analyzed for shear stress induced by torsion as well as normal stress from the bending moment. The normal stress calculation was made by estimating the skin as a two-flange structure and using equations from Reference 26. The maximum normal stress calculated was 52,000 psi at take-off. Evaluating this stress value over the wing-box cross-sectional area at the root, the maximum bending load was calculated to be  $4.27E7$  lbf.

Since the wing is a two-spar construction, the wing-box can be treated as a three-cell structure, consisting of the leading edge airfoil radius, mid-body and the trailing edge adjacent to the flaps. The maximum torsional shear stress was calculated by solving for the shear flows within the contours of the wing-box. Multiplying the shear flow values by the parameter thickness where they are applied, revealed the shear stresses. It was found that the maximum shear stress ( $\tau = 27,000$  psi), also at takeoff, was located at the mid-body section of the wing-box. The maximum torsional shear at that location is  $3.25E8$  lbf. Comparing the applied stresses to their respective material allowable stresses, for the skin, the normal stress controls. Therefore, the skin was sized according to the bending load requirements.

The spars are used mainly to support the inertial loads on the wing, such as the landing gear. The front and rear spars are analyzed as integrally machined C-sections. By designing the spar cap as a one piece structure, the production costs are reduced.<sup>24</sup> The C-section configuration was chosen to facilitate corrosion inspections without suffering the twisting of the Z-section design. The dimensions and materials are listed in Table ().

The six stringers are designed mainly as insurance for any skin failure. That is, the skin by itself is sized to resist the normal stresses. So each Z-stringer is designed to withstand 1% of the total bending

moment imposed on the skin. The Z-section configuration was chosen for the stringers to facilitate fabrication and to ease the possibility of water corrosion, since the Z-section is less likely to trap water than C-sections. Also since the Z-sections will be under a light load, a lesser tolerance to loading was considered acceptable.

The ribs play a vital role in distributing the applied loads among spars, stringers and skin. Ribs also help maintain skin rigidity. For stress analysis, a rib was estimated as a square structure composed of two flanges bounded by two webs. The rib only has one lighting hole rather than several small ones to reduce the stress concentrations within the rib and provides more space for fuel storage. The wing as a whole consists of nineteen ribs spaced at twenty inches. The rib at the root is sized to resist a maximum crushing load, shear, of 55,000 lbf.

Having sized the components of the main wing, the volume can now be calculated by numerically integrating the empty space between the skins using the trapezoidal approximation. The wing volume of the main wing section was calculated to be 14,000 ft<sup>3</sup>.

Now that the main section is done our attention was turned to the folding wing section. The folding wing section is made as a hollow structure consisting of skin and six ribs spaced at five foot intervals. Since the folding wing section is made up of a different material than the main section of the wing, a separate, but similar, stress analysis is required. The bending moment was calculated at 1.55E8 lbf-ft, which is 70% less than the bending moment at the root. Since the bending moments are the controlling loads on the wing, the loading of this wing section is much less than the main wing. The skin thickness at the hinged location of the folding wing section is 0.95 inches, which is considerably less than 3.2 inches at the root of the main wing.

### **12.3. Empennage**

The horizontal tail is designed as a two-spar structure which is reinforced with 18 ribs spaced at 2 ft. intervals, Figure 21. Since the horizontal tail does not carry fuel, there is not a lighting hole. This makes the ribs more structurally sound than those on the wing.

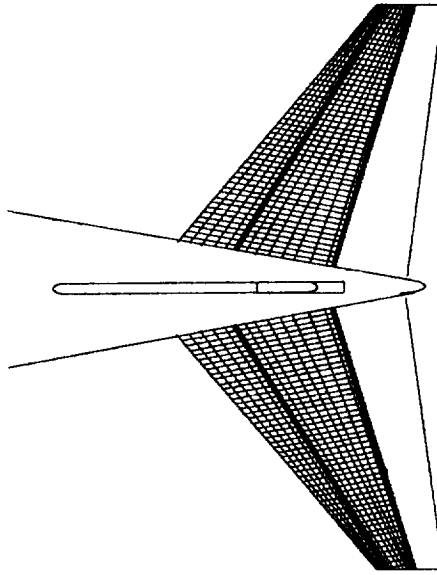


Figure 21. Structure of Horizontal Tail

The bending moment at the root on the horizontal tail is derived from the pitching moment. The aircraft has a tendency to pitch down, the horizontal tail must counteract this moment for steady flight.

From stability and control analysis, the pitching moment coefficient is  $-0.02$  and has a value of  $8.2E6$  lbf-ft. Knowing the distance to the center of gravity and assuming an elliptical force distribution on the tails, the resultant force on each tail is  $7.2E4$  lbf. This force is estimated to be 11 feet from the center of the two horizontal tails' intersection. From this the bending moment is calculated to be  $815,000$  lbf-ft at the root of the horizontal tail.

The normal stress was calculated by assuming the skin as a rectangular body with two webs bounded by two flanges. The applied stress of  $33,000$  psi is well under the material's allowable stress of  $52,000$  psi. Using  $1.5$  as the safety factor the horizontal tail's skin at the root was determined to be  $1$  inch.

The structure of the vertical tail is also controlled by stability and control. The vertical tail is sized for the worst case scenario of having one engine out. This situation would result in a yawing moment on the aircraft, which could render it unflyable.

The analysis assumes that the outboard engine has failed. The yawing moment is calculated by summing each engine's thrust at the cg. This resulted in a yawing moment of 6.7E6 lbf-ft with 100,000 lbf of thrust per engine. From this, the vertical tail skin size came to be 1.2 inches thick.as can be seen in Figure 22.

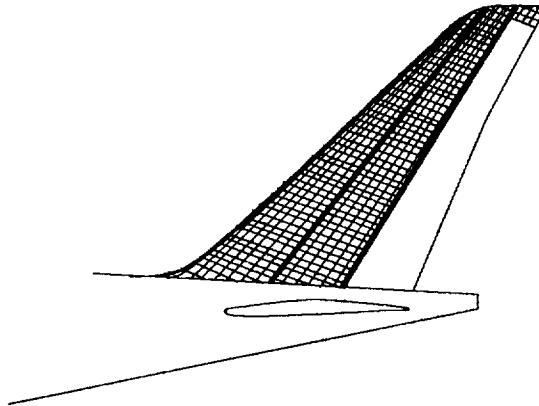


Figure22. Structure of Vertical Tail

#### 12.4. Fuselage

The fuselage shell is a semi-monocoqued circular structure composed of aluminum-lithium skin, supported by longitudinal stringers riveted to the skin. The stringer-type chosen is extruded Z-stringers. Z- sections have high structural efficiency and easy assembly. Figure {} shows the fuselage structural layout for the VLCT-13. The circular frames are set 22 inches apart with a depth of 9 inches. Figure 23 shows the longerons as spaced as 12 inches apart.

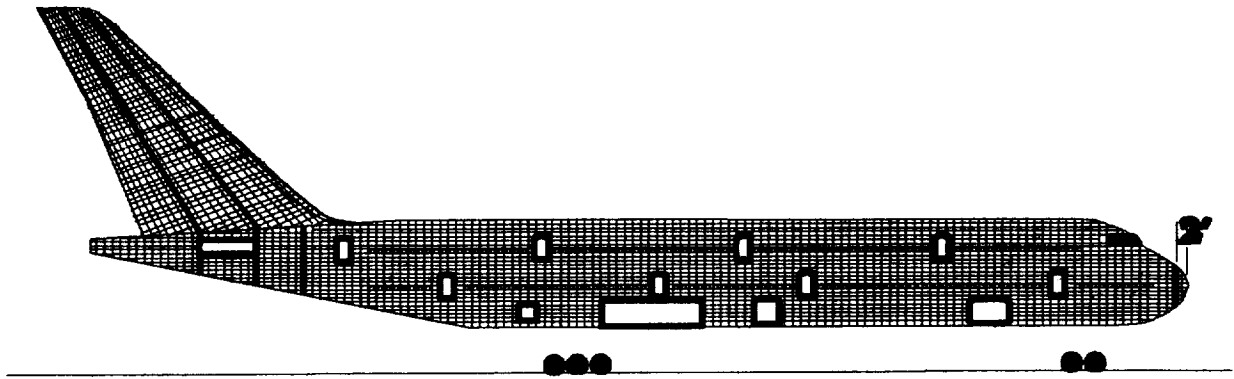


Figure 23. Fuselage Structure

Due to the close proximity of the fuselage shell to the root of the wing, the torsion caused by the lift at these two locations are almost equal in magnitudes. Therefore, to simplify the fuselage skin analysis without sacrificing too much accuracy, the torsion at that location is estimated to be 10% greater than at the wing root. With this assumption, the torsion at the fuselage is approximately  $2.20\text{E}8$  lbf-ft. The skin material is  $2.85\text{E}6$  lbf/ft<sup>2</sup>, with a factor of safety of 1.5 employed.

The minimum fuselage skin thickness required to resist the applied loads is calculated by estimating the fuselage cross-sectional area as being composed of two half circles and a rectangle at the center and solving for the shear flow.<sup>27</sup> Once the shear flow was calculated, the skin thickness was then calculated to be 2.92 inches.

A conventional fail-safe floor design is implemented. The floor consists of horizontal floor beams crossing axially to the sides of the fuselage, where each floor beam is bolted to a frame. Bolts are chosen over rivets as fasteners mainly because, in general, bolts show stronger resistance against fatigue and shear. In addition, since bolts are removable, whereas rivets are permanently fastened, maintenance and corrosion inspections are facilitated. At the cargo section, the floor beams are supported to frames and by floor struts. The interlocking beam-frame network is then covered by a stiffener-supported floor panel. The floor panel must be rigid enough to ensure that it does not warp or bend significantly which could damage the electrical circuitry located underneath the floor.



The floor loading analysis for the VLCT-13. Analysis was carried for every 22 inches of floor section in the longitudinal direction. This is appropriate because for stress analysis, the floor was modeled as a cantilever beam, so a boundary must be set for each floor panel in the longitudinal direction to make the approximation valid. In addition, a passenger seat is estimated to occupy 22 inches and the frame-supports are spaced at that dimension, making the boundary partition also convenient. The cross-sectional shape of the floor panel is approximated to be a square structure, composed of two flanges, bounded by two webs.

The transverse loads imposed on the floor panel section consists mainly of passenger and structural loads. Each passenger seat location is estimated to give a load of 250 lbf, while the structural loads at each floor is estimated to be 500 lbf.

The distributed load at the cargo section is approximated by a series of steps. First, the number of floor panels is calculated by dividing the fuselage length (180 ft.) by 22 inches. This gives 98 floor section panel units from forward to aft in the fuselage. The load for each floor panel is then calculated by dividing the baggage load (120,000 lbf) by the number of floor panels units. This gives a distributed load of 1333 lbf. Unlike the passenger floors, there are no spaces between loads in the cargo floor, making the distributed load reasonably accurate.

The actual method used in calculating the bending moments and shear on each floor utilized influence-diagrams, and shear and moment diagrams. The bending moments and shear forces are solved by multiplying the applied loads at each load point with the corresponding slope of the appropriate diagrams.

The final results of the bending moment and shear force analysis, as expected, the greatest loads are imposed on the cargo section ( $M_b = 75,000 \text{ lbf-ft}$ ;  $V=19000 \text{ lbf}$ ). As was done for the wing section, the applied normal stress was calculated to be  $1.2\text{E}5 \text{ psi}$ .

### **13. MANUFACTURING**

The VLCT-13 is constructed mainly of the following materials: Aluminum-Lithium, Aluminum 7075-T6, Graphite-Epoxy and Steel H-11, with Al-Li being the primary material. Al-Li will be bought in volumes of continuous sheets, since it is used as exterior cover for the aircraft and close tolerances would not be necessary, this should prove to be cost-effective. The Al-7075-T6 and Steel H-11 materials will be bought in large quantities fabricated as beams.

Figure 24 shows the assembly breakdown for the VLCT-13. The aircraft will be assembled in sections. The constant-area fuselage is made up of four sections, with two sections being equal to each other to reduce manufacturing costs. The two different sizes come about to facilitate mating of the fuselage and wing box. The fuselage sections are connected together with rivets first, so that installation of the electrical systems could be facilitated. Next, the wing and empennage are connected to the fuselage, then the engine and landing gear will be installed last.

The VLCT-13 will require cooperation between airframers, engine manufacturers and laborers to become a successful viable aircraft. An aircraft of this size could not be financed by one airframe company alone. Cooperation between US. airframers and those abroad will be needed before the VLCT-13 can become an economically viable possibility.

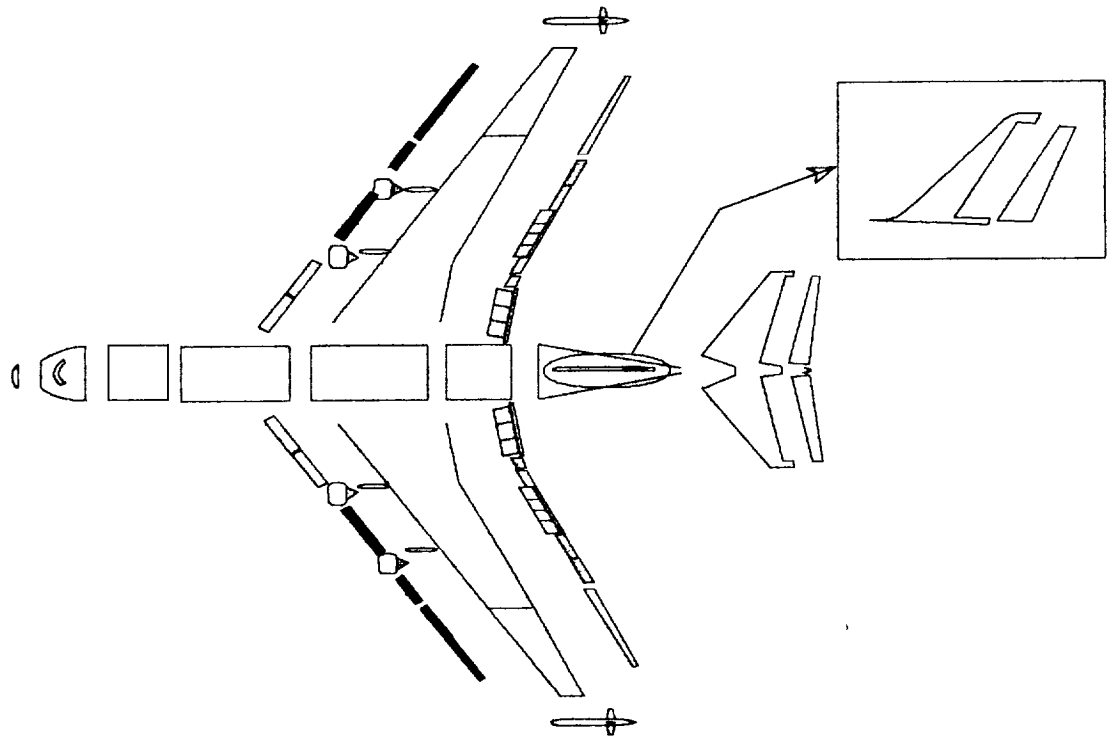


Figure {}. Manufacturing Breakdown

## 14. LANDING GEAR DESIGN

### 14.1. Landing Gear Location and Load Distribution

The placement and sizing of the landing gear system for the VLCT-13 was based on the most adverse conditions. These conditions include center of gravity shift and maximum design gross weight. Figure 25 shows the positions of the forward and aft center of gravity limits relative to the nose; 132 ft. to 145 ft. respectively. From the weight sizing, gross weight of the aircraft attains a maximum value of 1.4 million pounds when it is fully fueled for a 7,000 nm journey, transporting 800 passengers with 30,000 pounds of cargo.

The VLCT-13 landing gear system is similar to that of the Boeing 747 in that there will be five struts. There is one nose gear strut and four main gear struts; two of the main struts are lodged beneath the wing near the root and the remaining two are situated at the fuselage belly, Figure 1. Using the information in the previous paragraph and the method outlined in the diagram below, the load on each gear strut and its location relative to the nose is obtained.

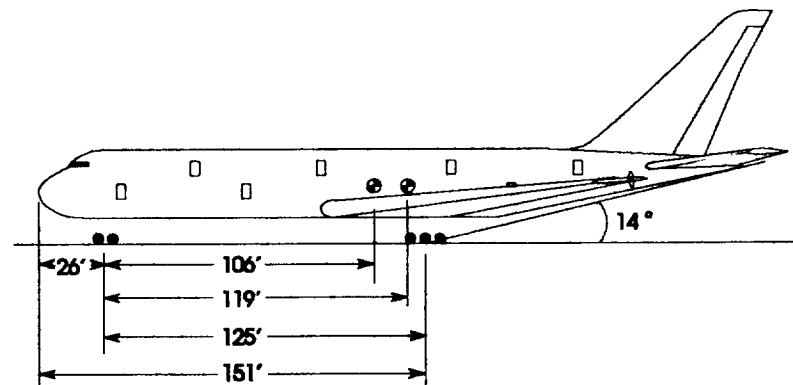


Figure 25. Landing Gear Locations

Values for the nose and main gear strut locations were chosen arbitrarily with the following considerations in mind:

- a. Excluding any safety factors, the main gear would assume 90% of  $W_{TO}$ .
- b. The minimum load on the nose gear should be more than 6% of  $W_{TO}$  for steering purposes.

- c. The main gear should be positioned such that the rotation angle of the aircraft on takeoff is  $15^{\circ}$ .

In addition to considerations listed above, placement of the wing landing gear on the rear spar is convenient from a structural standpoint. Placing the wing gear strut ahead of the rear spar would result in a reduction of wing box strength near the root; the ribs in this region would have to be removed to accommodate the strut. On the other hand, placing the wing gear aft of the rear spar requires implementation of a frame to support the struts. This would increase the weight of the aircraft and reduce fuel volume or space for other accessories.

Using the nose of the aircraft as a reference point, various combinations of nose gear and main gear locations were examined. It was observed that by placing the nose gear strut at 26 ft. and placing each main gear strut at 151 ft., the most satisfactory load distribution was attained. Furthermore, at a value of  $14.6^{\circ}$ , the rotation angle was reasonable. With the longitudinal placement of the main gear determined, the lateral distance from the wing root to the rear spar was calculated. As a result, each wing gear strut is positioned 19 ft. from the centerline of the fuselage. Figure 26 serves as a summary of results; it shows the longitudinal and lateral dimensions of each landing gear strut, the resulting load distribution, and the landing gear placement relative to the forward and aft center of gravity locations. It should be noted that the loads shown accommodate a safety factor of 1.07 in accordance with FAR 25 regulations; therefore, the total load supported by the five struts represents 107% of the maximum aircraft landing weight. In this section on landing gear design, the term "total load" will refer to 107% of  $W_{Land}$ .

The maximum load on the nose gear is 213,000 lbf; hence, the nose gear supports as much as 14% of the total load. The minimum load is 67,500 lbf, or 5% of the actual aircraft load of 1.4 million pounds. This is well below the preferred minimum of 8%  $W_{TO}$ . However, it is acceptable; the DC-10 is known to sustain a minimum nose gear load which is also 5% of its take-off weight. Each of the four main gear struts supports an equal portion of the  $W_{TO}$ . This implies that each of the four struts supports 333,000 pounds and 89% of the total load.

As indicated in Figure 27, the main gear is slightly staggered so that the fuselage gear struts are six inches aft of the wing gear struts. This is done primarily to increase the tail-down angle to the preferred 15°. Furthermore, this reduces the risk of damaging concrete runways.

## 14.2. Tire Selection and Wheel Arrangement

The dominant parameter in choosing the type of tire for the nose gear strut was "maximum allowable load". The maximum static load on the nose gear strut is 213,000 lbf; however, the maximum dynamic load on the nose gear is 293,000 lbf. A likely candidate was discovered from examining B.F. Goodrich tire data charts. The tire chosen has a maximum load capability of 76,000 lbf.

Table 14-1. Nose Gear Tire Data

Maximum Loading	76,000 lbf
Outer Diameter	56 in
Width	16 in
Inflated Pressure	315 psi
Loaded Radius	24.1 static in
Loaded Radius	18.7 flat in
Ply Rating	38

The maximum dynamic load, using four of these tires, would be 73,000 lbf per tire. This would be enough to support the most adverse nose gear load. A major disadvantage of this tire is the pressure, 315 psi. Consequently, using the LCN Method outlined in Reference 29, this results in an LCN of 112; hence, the VLCT-13 would only operate at airports with an LCG of 1. An alternate approach would be to increase the number of tires at the nose gear so that smaller tires could be used. This would lower the dynamic load per tire, lower the LCN significantly, and enable the aircraft to operate at more airports. However, a large number of tires would not facilitate steering and scrubbing would occur. Also, fitting the nose gear into the fuselage would be difficult with a large number of tires.

Each of the main gear struts will have six wheels. Therefore, the maximum static load per tire is 55,500 pounds. Based on the same tire data charts, there were two likely candidates; one had a maximum load capability of 57,800 pounds, a width of 20.5 inches, and an inflation pressure of 185 psi. The other was capable of a 58,000 lb maximum load; however, the inflation pressure was 250 psig at a width of 26 in. The

57,800 lb tire was chosen for its smaller width and inflation pressure, since there is no significant difference in load capability. Data for this tire is given in Table 14-2.

Table 14-2. Main Gear Tire Data

Maximum Loading	57,800 lb
Outer Diameter	52 in
Width	20.5 in
Ply Rating	34
Inflation Pressure	185 psi
Loaded Radius	21.3 static in
Loaded Radius	14.3 flat in

The tire footprint of the aircraft is shown in Figure 27. The four wheels of the nose gear strut form a dual tandem bogey arrangement. Inspection of the imprint left by the main gear tires reveals tri-tandem arrangement among each of the four struts. With twice as many wheels as in the case of the nose gear strut on a Boeing 747, the contact area is hence larger. The tires on the nose gear of a Boeing 747-300 are 20 inches wide, and the total contact area from the two tires is 522 square inches. The total contact area of the tires on the nose gear of the VLCT-13 is 334 square inches. The increased contact area combined with the twin tandem arrangement makes steering difficult and causes the tires to scrub against the runway. This problem is addressed by having the steering column of the nose gear strut attached to the front axle. In effect, steering capability is placed on the front wheels and the rear wheels on the nose gear strut follow through. To prevent scrubbing on the main gear wheels, the front wheels on each wing gear strut rotate with the front wheels on the nose gear strut. Differential braking is another approach in preventing scrubbing on the main gear wheels. As the nose gear is being turned, the brakes can be applied to three wheels on either side of each wing gear strut.

### 14.3. Turning Radius

With the wingspan of the aircraft at 305 ft. and an overall length of 275 ft., the two major concerns arose. Can a  $180^\circ$  turn be executed on a 150 ft. wide runway. Will VLCT-13's wingspan interfere with aircraft on taxiways and runways? Figure 28 shows the turning radius of the VLCT-13. With a steering angle of  $60^\circ$ , a  $180^\circ$  turn can not be performed on a 150 ft. runway. As observed in Figure 28, the turning center

is 72 ft. from the centerline of the fuselage. Therefore, with the distance between the nose gear and the wing gear struts being 125 ft., the wheels of the nose gear and the wing gear would be off the runway after the aircraft rotated  $90^\circ$ . In the case of a 150 ft. runway, increasing the steering angle would not be a solution because the distance between the nose gear and the wing gear is too long and the wing gear struts are too far apart. If the runway were 200 ft. wide, a  $180^\circ$  turn could be performed. However, the steering angle would have to be  $75^\circ$ . For this reason, the aircraft is equipped with the steering system that is typical of the Boeing 727. It incorporates both hand wheel steering and rudder pedal steering and is hydraulically powered. Steering angles as high as  $78^\circ$  can be attained.

As seen in Figure 28, the outermost wing tip of the aircraft can extend as far as 225 ft. from the turning center. This distance can be decreased by increasing the steering angle and having the wing tips fold up so that the wingspan reduces to that of the Boeing 747-400. For instance, with a steering angle of  $78^\circ$  and the wing tips folded, the outermost portion of the wing extends 132 feet from the turning center.

#### **14.4. Tip-over Criterion**

As mentioned previously, the rotation angle of the aircraft is at take-off is  $15^\circ$ . This satisfies the rotation angle criteria for the case of static deflection only. Two other cases of concern involve the main gear struts in the compressed and extended positions. Figure 29 below shows how the rotation angle changes as the strut travels from a compressed state to an extended state. When the strut is compressed after initially being in its static state, the strut travel is 5.2 inches. The rotation angle decreases to  $15^\circ$ . When the strut is in an extended position, the strut travel is 10.4 inches. The rotation angle increases from  $15.2^\circ$  to  $15.6^\circ$ . Therefore, the tail-down angle does not change significantly as the strut leaves its static state and is kept within  $12^\circ$  to  $15^\circ$  bracket.

#### **14.5. Retraction Kinematics**

The nose gear consists of an oleo-pneumatic strut 8.5 feet high and 1.4 feet in diameter. Figure 26. It is accompanied by a drag brace situated at  $45^\circ$  with respect to the centerline of the strut. This brace helps to absorb the high static and dynamic loads experienced during landing. Figure 26 shows how the nose gear is



retracted. The oleo-pneumatic strut retracts forward into the fuselage. As this is done, the drag brace folds inward toward the strut with the aid of torque links. Because there is only a 6 foot clearance between the bottom of the fuselage and the cargo ceiling and each tire has a diameter of 56 inches, the wheel truck rotates so that all four tires rest on the fuselage floor. This is actuated by torque links extending from the front axle. The nose gear strut has free-fall capability since it retracts forward. The uplocks can be manually released and gravity pulls the gear down until it is fully extended and locked into position.

The wing gear is very similar to that of the Boeing 747-400 in that they have similar components and the manner of retraction is the same. The sustained load is distributed among the main oleo-pneumatic strut, the drag brace and the side strut. The main strut is attached to a trunnion, which, in turn, is attached to the rear spar of the wing. Figure 26 shows the retraction of the wing gear strut. The side strut is pulled inward until it rests against the oleo-pneumatic strut. An actuator retracts the gear inward so that in an uplocked position, it is at right angles to its extended, down locked position. When retracted, the entire strut assembly lies within the yehuti and the wheel truck rests within the fuselage. There is a six inch between the outer wheels of the fuselage gear and the bottom of the wheels of the wing gear strut; Figure 26 shows this relationship. These wing gear struts have free-fall capability; as with the case of the nose gear, manually releasing the uplock allows gravity to pull the strut down to an extended position.

Since there are six tires on each fuselage gear strut, it is not possible to retract it forward. There is not enough clearance because of the wing box spars. Hence, as shown in Figure 26, the wheels are retracted straight up. This is done with telescopic landing gear. The total length of the strut when fully extended is 11 feet. The strut is divided into five sections: the top two sections are 2.5 ft. long and the remaining three sections are 2 ft. long. Each section rotates into the section directly above it until the top section rests directly above the wheel-truck. In effect, the strut length, after retraction, reduces to 2.5 feet.

# FOLDOUT FRAME

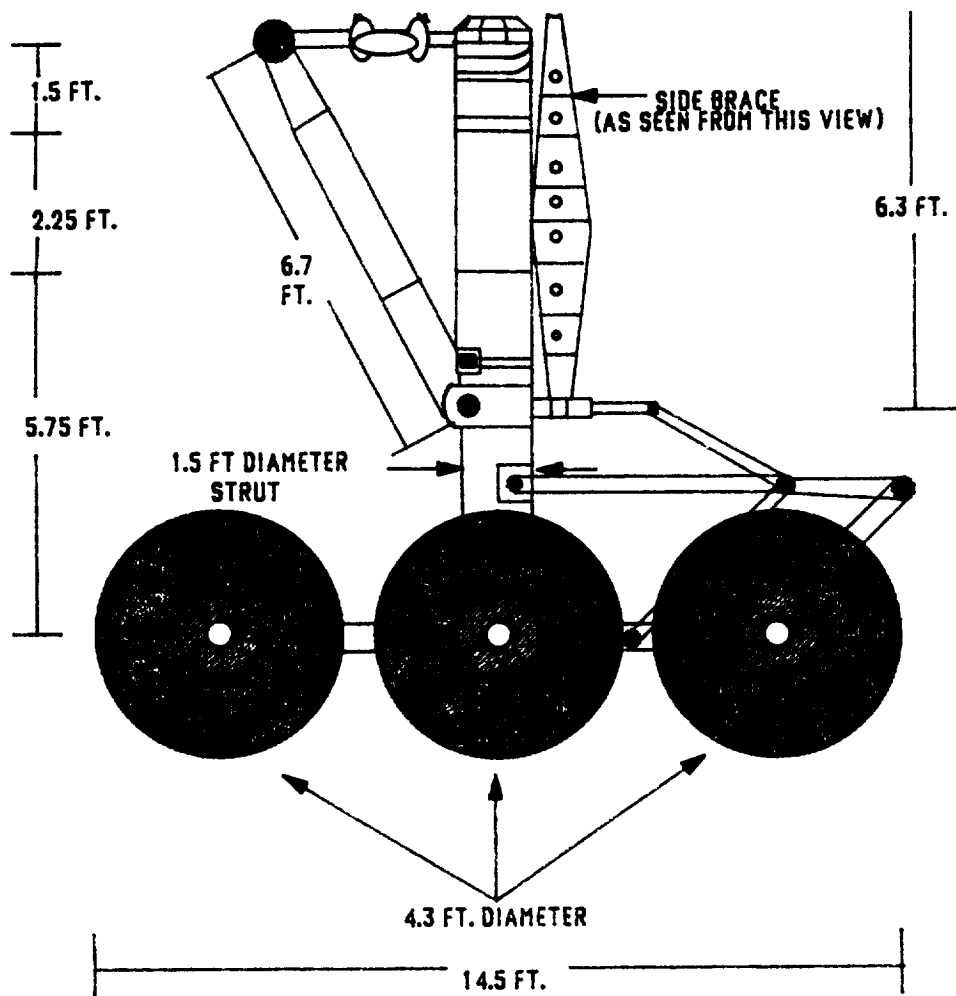
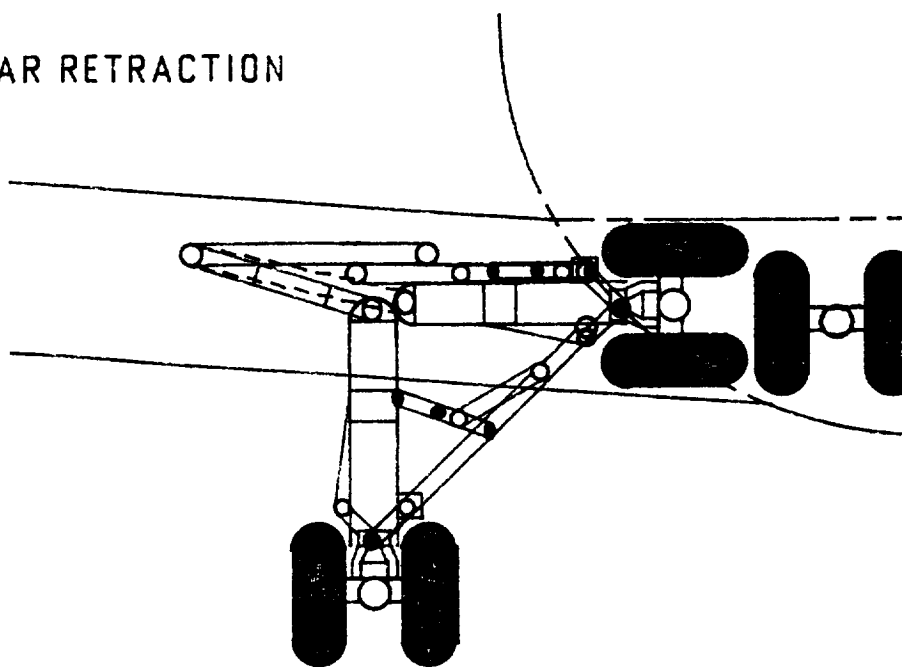


FIGURE 2: WING GEAR STRUT WITH DIMENSIONS

## WING GEAR RETRACTION



2.

FOLDOUT FRAME

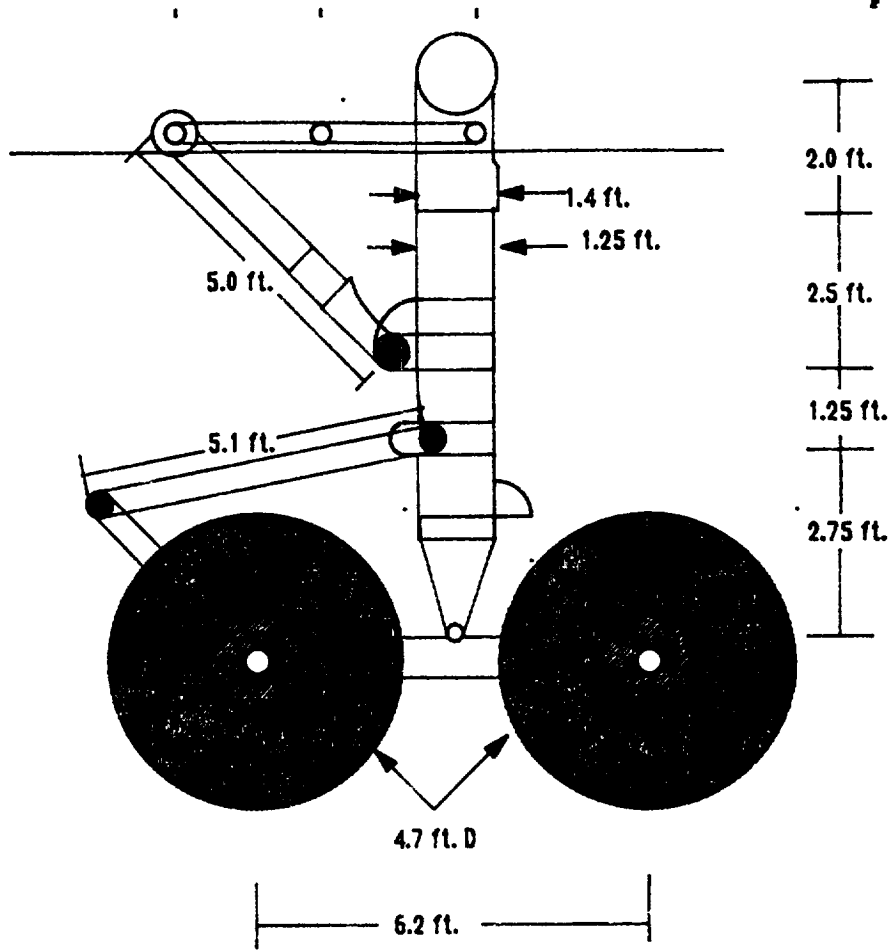


Figure 25: Nose Gear Strut with Dimensions

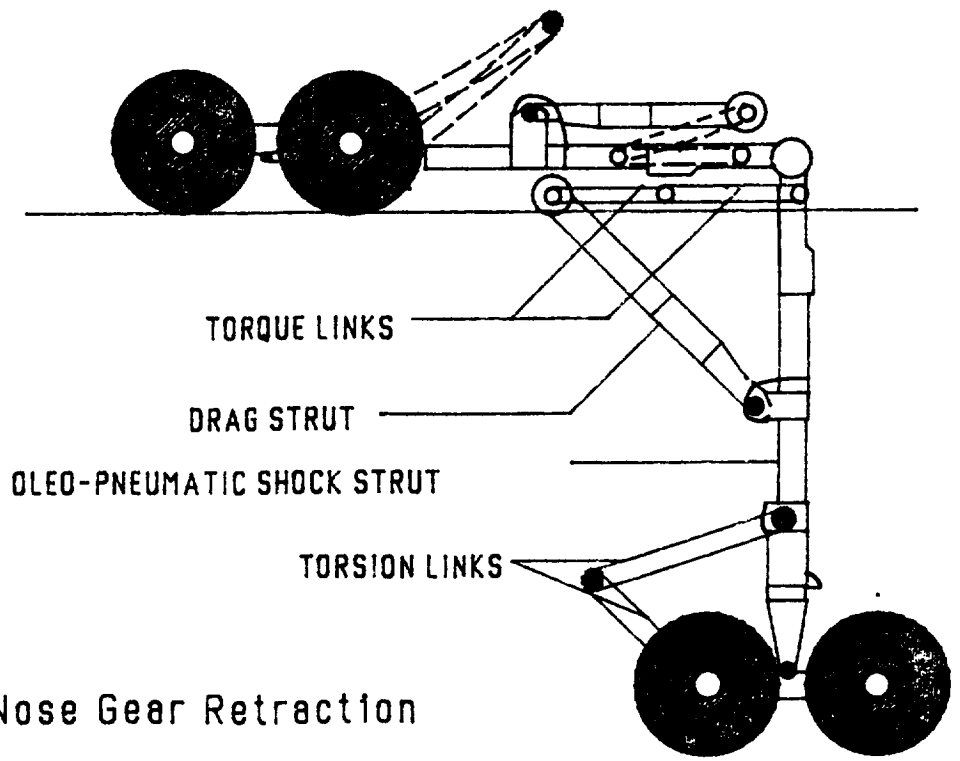
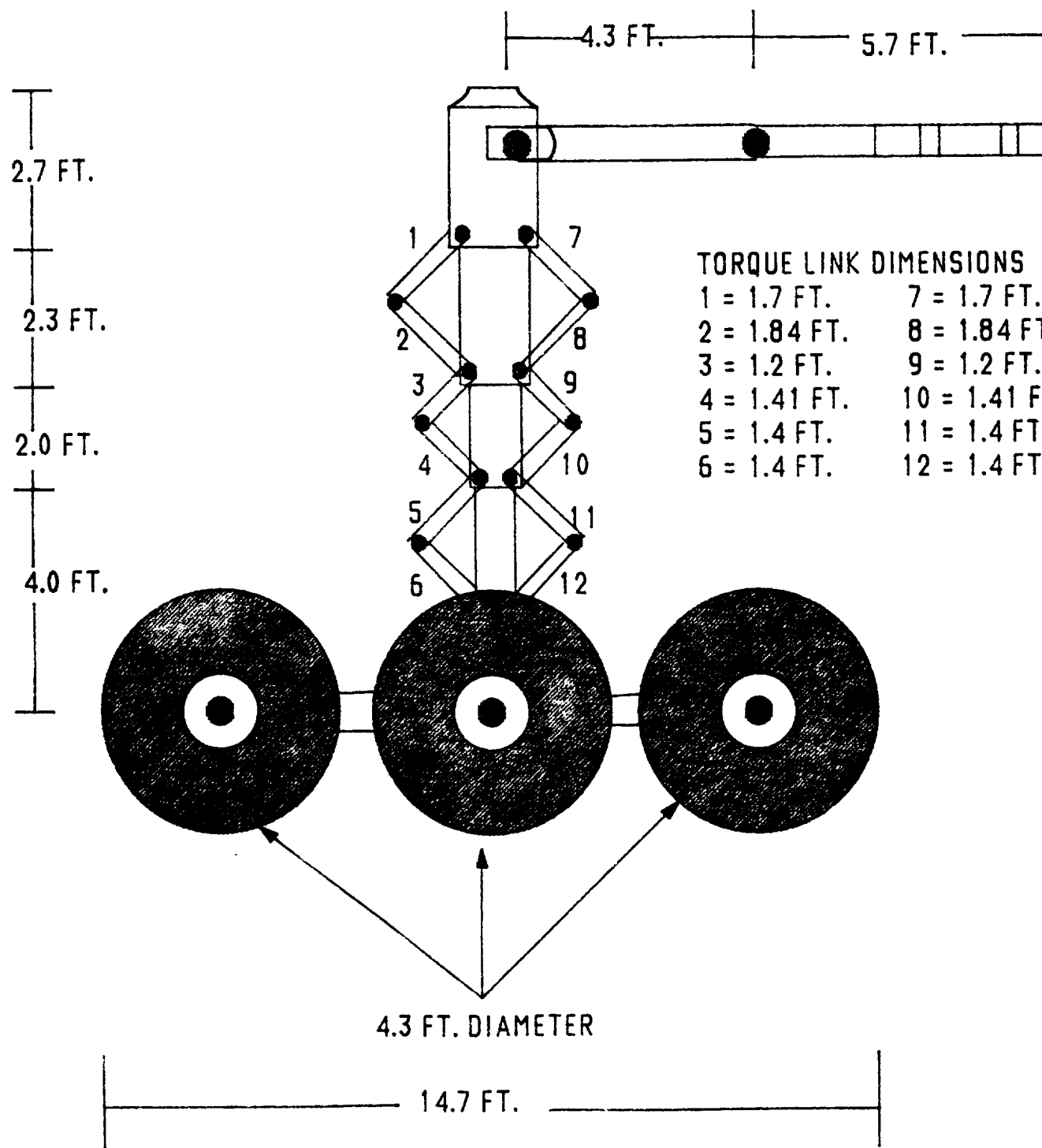


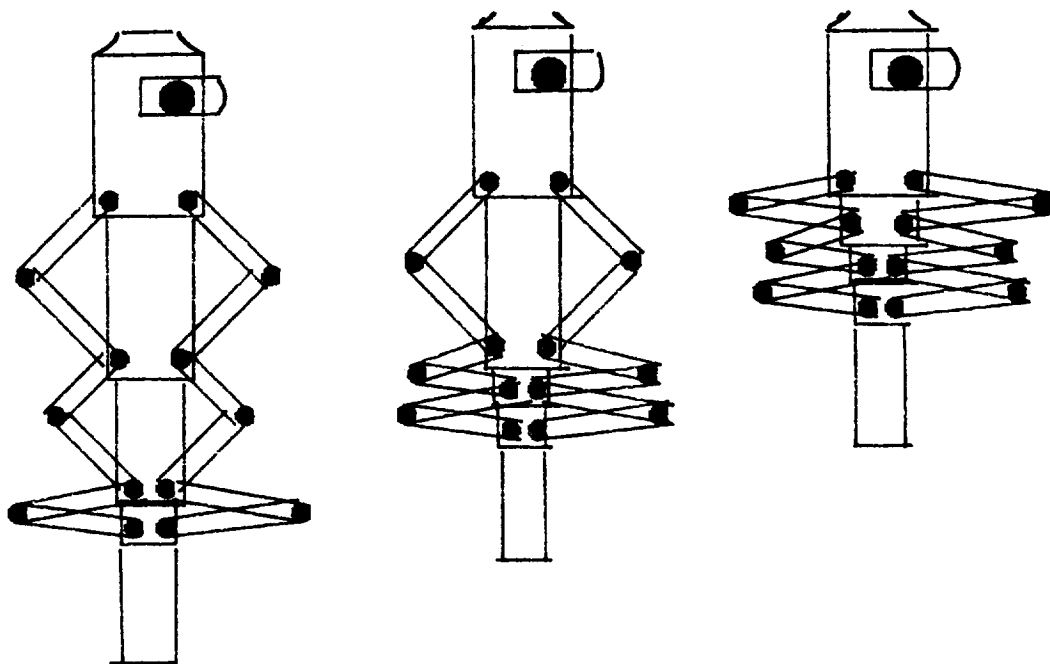
Figure 26: Nose Gear Retraction

6.  
**FOLDOUT FRAME**

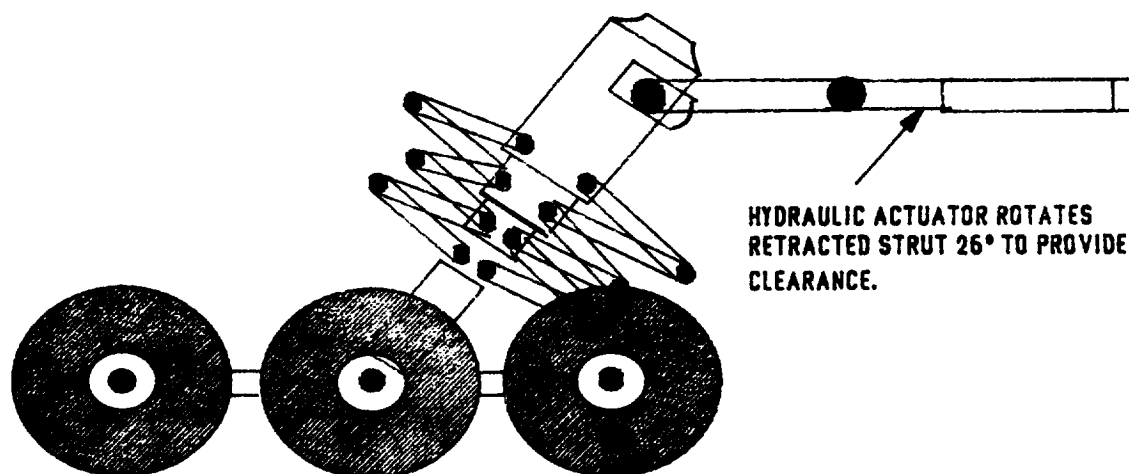


**FIGURE 2: FUSELAGE GEAR STRUT LAYOUT.**

2.  
FOLDOUT FRAME

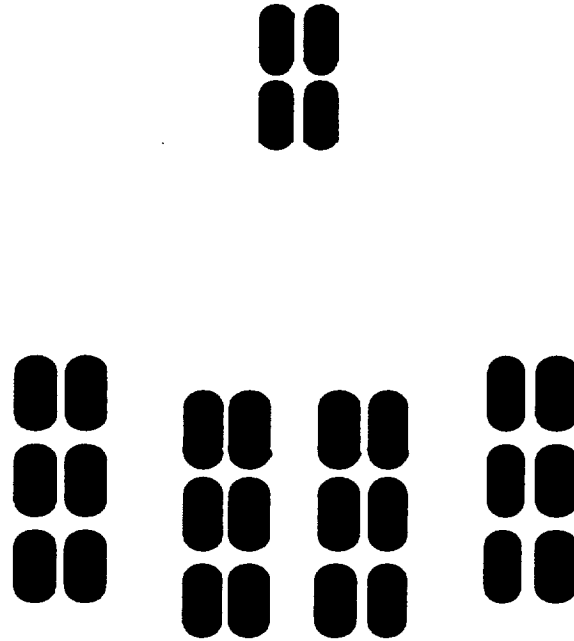


RETRACTION SEQUENCE OF FUSELAGE STRUT.



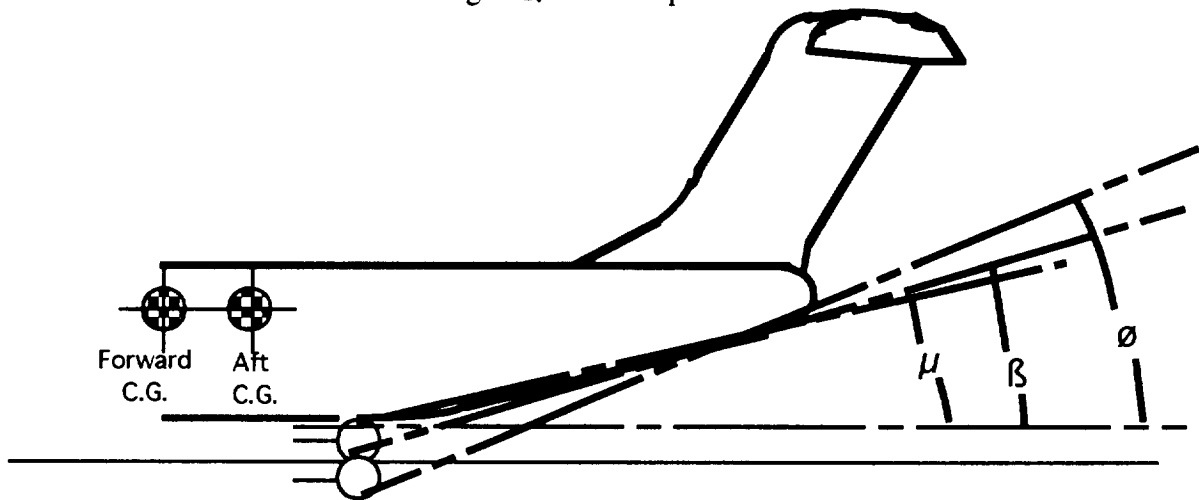
POSITIONING OF STOWED FUSELAGE GEAR STRUT.

FIGURE 2. FUSELAGE GEAR RETRACTION.



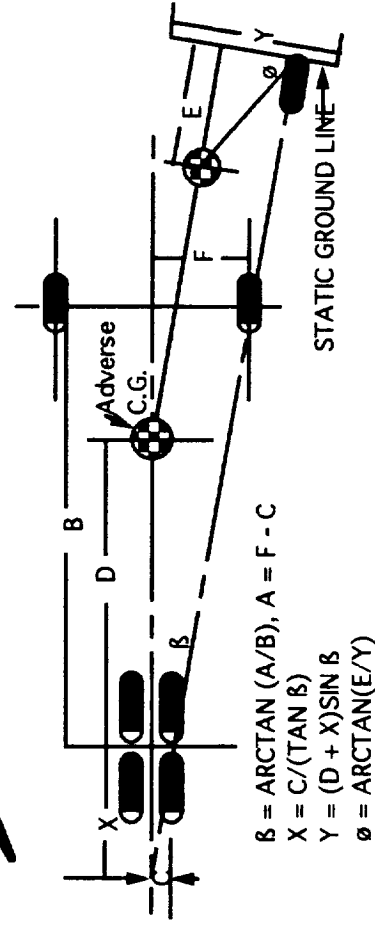
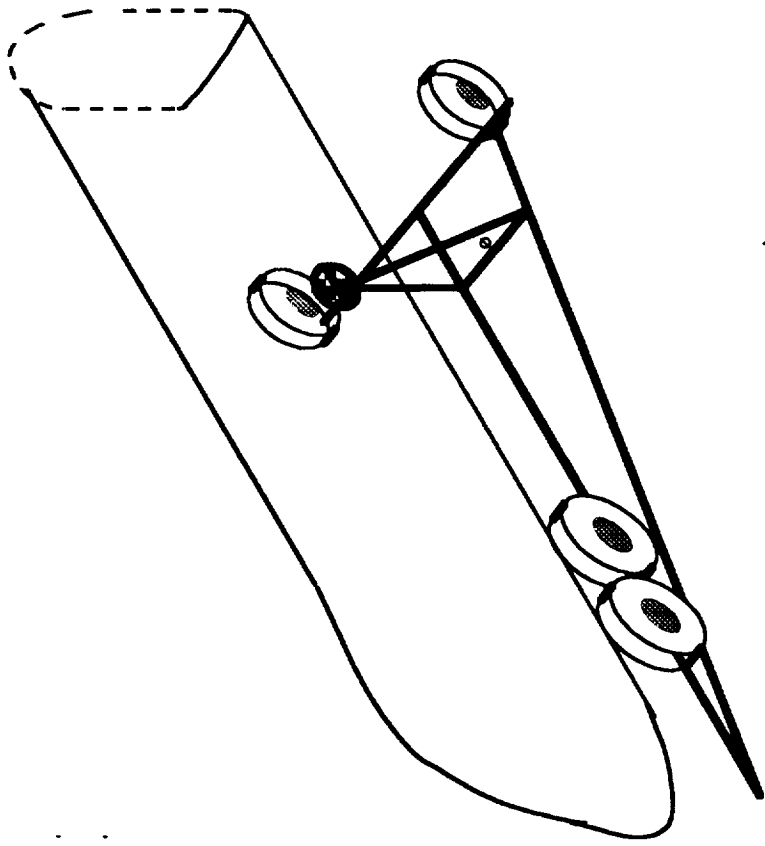
TIRE FOOTPRINT OF VLCT-13 LANDING GEAR SYSTEM.

Figure 27: Tire Footprint



$\mu$  = Rotation Angle When Strut is Compressed.  
 $\beta$  = Rotation Angle When Strut is in Static Position.  
 $\phi$  = Rotation Angle When Strut is Extended.

Figure { } Tail - down Angles.



$$\begin{aligned} B &= \text{ARCTAN}(A/B), A = F - C \\ X &= C/(\text{TAN } B) \\ Y &= (D + X)\text{SIN } B \\ \phi &= \text{ARCTAN}(E/Y) \end{aligned}$$

Figure 29 Turnover Angle Calculation.

## **15. CONCLUSIONS AND RECOMMENDATIONS**


### **15.1. Conclusions**

With an expanding world economy, the business and tourist industry along the Pacific Rim is expected to increase dramatically by the turn of the century. Airlines require an 800 PAX, long-haul airplane to satisfy the increased passenger demand expected in the 21st century. The VLCT-13 is a large version of a conventional, tried and true design with one marked difference, the VLCT-13 is a VERY large commercial transport able to fly 7000 nm carrying more than 800 PAX. With a 2.7 cent DOC/PAX-seat mile, the VLCT-13 is competitive with current airplanes. An initial investment of \$195 million 1993 US dollars per airplane introduces a competitor and successor to the B-747 at a lower operating cost.

### **15.2. Recommendations**

A thorough study of passenger egress from the upper deck is required to justify the VLCT-13 design. An actual cross section should be built to determine if the tall emergency slides affect passengers physically and mentally.

Study a design of a large single deck fuselage with an integrated wing. A double deck design is questionable from a safety standpoint. The emergency slides from the upper deck are very long and possibly too dangerous. A single deck fuselage, since it would have to be flat and very wide, could contribute lift and therefore decrease wing area and span. The landing gear could be spread out more to decrease damage to runways because of the weight. Reference 28 explores several design concepts including an flat, integrated wing design.<sup>28</sup>





## REFERENCES

1. Irvine, Clive, "Wide Body", *Air & Space*, December 1992/January 1993, pp. 78 - 86.
2. Ott, James, "Competition to force new airline structures", *Aviation Week & Space Technology*, March 15, 1993, p. 65.
3. Kandebo, Stanley W., "Stable Engine Sales seen in late 1994", *Aviation Week & Space Technology*, March 15, 1993, p. 78.
4. Butterworth-Hayes, Philip, "Europeans to be major partners in 800-seater development", *Aerospace America*, April 1993, pp. 12 - 13.
5. Van't Riet, Robert, "RFP for a New 800 Passenger Transport Commercial Aircraft", Cal Poly, SLO, Senior Aircraft Design Class, November 4, 1992.
6. Waters, M., Ardema, M., Roberts, C., Kroo, I., "Structural and Aerodynamic Considerations for an Oblique All-Wing Aircraft", AIAA 92-4220, August 24-26, 1992/Hilton Head, SC.
7. Jones, Robert T., "The Oblique All-Wing Airplane", NASA Ames Research Center.
8. Bagely, J.A., "Some Experiments on an Engine Installation Above the Wing of a Swept-Wing Aircraft", Royal Aircraft Establishment. Technical Memorandum Aero 1271. November 1970.
9. Cable TV Networks commercial , TWA, April 1993
10. USA Today, February 20, 1993
11. Boeing 777 pamphlet
12. MD-12 reference binder
13. Roskam, J., Part VIII: Airplane Cost Estimation: Design, Development, Manufacturing and Operating, Roskam Aviation and Engineering Corporation, 1989.
14. RDS Student. Raymer Design Program for IBM.
15. Roskam, J., Part II: Preliminary Configuration Design and Integration of the Propulsion System, Roskam Aviation and Engineering Corporation, 1989.
16. Shevell, Richard, Fundamentals of Flight, Prentice-Hall, Englewood, NJ, 1989.
17. Roskam, J., Part VI: Preliminary Calculation of Aerodynamic, Thrust, and Poer Characteristics, Roskam Aviation and Engineering Corporation, 1989.
18. Rolls-Royce pamphlet
19. "105,400-lb. Thrust Reached in GE90 Test", *Aviation Week & Space Technology*, April 12, 1993.
20. Patterson, Jr., James C.; Flechner, Stuart G., "Exploratory Wind-Tunnel Investigation of a Wingtip-Mounted Vortex Turbine for Vortex Energy Recovery", NASA-TP-2468, Langley Research Center Hampton, VA, 1985.

21. Andersen, Jr, John D.. Introduction to Flight, McGraw-Hill Publishing Company, 1989
22. The USAF Stability and Control Digital Datcom, Technical Report AFFDL-TR-76-45.
23. Roskam, J., Part VII: Determination of Stability, Control and Performance Characteristics: FAR and Military Requirements. Roskam Aviation and Engineering Corporation, 1989.
24. NIU, Mi, Airframe Structural Design. Commilit Press Ltd., LA. CA, April 1989.
25. Roskam, J., Part V: Component Weight Estimation, Roskam Aviation and Engineering Corporation. 1989.
26. Raymer, Daniel P., Aircraft Design: A Conceptual Approach. AIAA Incorporated. Washington, D.C., 1989
27. Riley, William F.; Zachary, Loren, Introduction to Mechanics of Materials. John Riley & Sons. Inc., NY, 1989
28. Das, Robert; Das, Rudolf, "Search for Successors to the Boeing 747". Wolken Ridder: A Magazine for KLM Staff, 20 February, 1993.